

Lightning Occurrence in Pukaskwa National Park and Surrounding Area.

Submitted in partial fulfillment of the requirements of the Master of Forestry Report.
Faculty of Forestry and the Forest Environment
May 10, 2000
Angus Carr (c)

ProQuest Number: 10611499

All rights reserved

INFORMATION TO ALL USERS

The quality of this reproduction is dependent upon the quality of the copy submitted.

In the unlikely event that the author did not send a complete manuscript and there are missing pages, these will be noted. Also, if material had to be removed, a note will indicate the deletion.



ProQuest 10611499

Published by ProQuest LLC (2017). Copyright of the Dissertation is held by the Author.

All rights reserved.

This work is protected against unauthorized copying under Title 17, United States Code
Microform Edition © ProQuest LLC.

ProQuest LLC.
789 East Eisenhower Parkway
P.O. Box 1346
Ann Arbor, MI 48106 - 1346

Abstract

Carr, A.P. 2000. Lightning occurrence in Pukaskwa National Park and surrounding area. Masters of Forestry Report: Faculty of Forestry, Lakehead University. 75 pp.

Keywords: lightning, fire occurrence, kernel analysis, Pukaskwa National Park, fire weather.

Pukaskwa National Park has implemented a natural fire regime emulation program. One component of the natural fire regime is the pattern of ignitions, primarily from lightning. There were three ways in which patterns of lightning strikes were investigated: a geographical analysis, a fire weather analysis, and an ignition analysis. The analysis for the first two components was carried out using a kernel analysis, which is a non-parametric probability density estimation technique. In the geographic analysis, probability of lightning strikes was tabulated by characteristics of the landscape- vegetation, topography, ecodistrict, and proximity to Lake Superior. It was shown that there was a strong effect of the proximity to Lake Superior- areas near the lake have a higher probability of lightning strikes than areas inland. The topographic component showed that high points on the landscape were more likely to get struck than the rest of the landscape. Other effects were masked by the effect of proximity to Lake Superior. In the fire weather analysis, probability density surfaces were prepared from the daily weather and from the weather on the day of lightning strikes. Strikes are most frequent at values of the Fine Fuel Moisture Code (FFMC) and Duff Moisture Code (DMC) that are not conducive to the ignition and survival of fire. The exception to this was a storm in June, 1995 which happened at a high value of FFMC and DMC. This storm presumably lit Fire Wawa 41/95. The ignition analysis was carried out as an anecdotal discussion of conditions at the time of ignition of the two fires that were ignited in the three years under study (1994-1996). The conditions surrounding these two ignitions, both in June of 1995, were consistent with other descriptions of fire weather in the Pukaskwa area. Warm and dry weather with a high barometric pressure preceded a lightning storm. The geographic analysis suggested that there might be relatively little reason to modify fire policy based on lightning density within the park. The weather analysis suggested that it is rare to have the right combination of events that might ignite fires- dry fuel and lightning.

Table Of Contents

Abstract	ii
Table of Contents	iii
Table Of Tables	v
Table Of Figures	vi
Introduction	1
Objectives	2
Literature Review	3
Lightning	3
Negative CG lightning	3
Positive CG lightning	4
Other processes in lightning flashes	5
Summary of the Lightning Process	6
Lightning-Caused Fire Ignition	6
Lightning Detection Systems	7
Lightning Ignition Prediction	9
Fire Weather (FWI)	9
Ignitability of Fuels	11
Lightning Weather Patterns	11
Analysis of Lightning Data	12
Lightning strike density and distribution	13
Probability Density Estimation	13
Setting	22
Data Sources	24
Lightning Detection System Data	24
Weather	25
Ignition Locations and Times	25
Vegetation Coverage	25
Topographical Information	27
Ecodistrict Information	27

	iv
Distance from Lake Superior Data	27
Data Coverage	27
Methods	30
Section 1 - Where?	30
Data Preparation	30
Analysis	31
Section 2 - When?	32
Section 3 - Fires	34
Software	34
Results	36
Section 1 - Where?	36
Probability Density Maps	36
Topographic Class Maps	39
Crosstabulations	39
Section 2 - When?	48
Daily Weather Probability Density	48
Lightning Weather Density	50
Section 3 - Fires	52
Fire 41	52
Fire 33	56
Discussion and Conclusions	59
Informal Examination	59
Section 1 - Where?	59
Section 2 - When?	61
Section 3 - Fires	62
Suggestions for Possible Future Research	64
Probability of Fire Ignition	64
Strikes on Exposed Ledges	64
References	66

Table Of Tables

Table 1: Vegetation classification system from a classification of satellite imagery of Pukaskwa National Park and area.	26
Table 2 - Table of distances to lightning detection system direction finders (DFs) to the three corners of Pukaskwa National Park.	40
Table 3 - Crosstabulation of the probability density maps with topographic class maps for both all strikes and positive strikes.	43
Table 4 - Crosstabulation of the probability density maps with peak class maps for both all strikes and positive strikes.	45
Table 5 - Crosstabulation of the probability density maps with the vegetation class map for both all strikes and positive strikes.	45
Table 6 - Crosstabulation of the probability density maps with the ecodistrict class map for both all strikes and positive strikes.	47
Table 7 - Crosstabulation of the probability density maps with the map of distance from Lake Superior for both all strikes and positive strikes.	47
Table 8 - Soldier Mountain weather station daily data at noon for the period from June 15 to June 30, 1995.	54
Table 9- Fuel types in a 400 ha square around the reported location of Fire 41.	54
Table 10- Fuel types in a 400 ha square around the reported location of Fire 33.	57

Table Of Figures

Figure 1 - Schematic diagram of kernel estimator process.	15
Figure 2 - The effect of smoothing parameter choice on density estimates.	16
Figure 3 - Three kernel estimators of a known distribution, using 1000 samples from the distribution described in the text (Equation 4).	18
Figure 4 - Simulated bivariate probability density field, in two dimensions.	19
Figure 5 - Local Setting of Pukaskwa National Park.	23
Figure 6 - The five ecodistricts of Pukaskwa National Park.	28
Figure 7 - Areal extents of individual data sets used in this project.	29
Figure 8 - Simplified description of how the smoothing factor was calculated for the preparation of the lightning density maps.	32
Figure 9 - Distribution of strikes by strength and polarity scores.	37
Figure 10 - Probability density map of all lightning strikes.	38
Figure 11 - Probability density map of positive polarity lightning strikes.	38
Figure 12 - Elevation map converted into 7 elevation classes of equal width.	41
Figure 13 - Peak elevation map derived from the elevation map using a maximum filter and map algebra.	42
Figure 14 - Probability density surfaces in the FFMC-DMC coordinate system.	49
Figure 15 - The locations of the two fires discussed in the text in relation to the Park boundary.	53
Figure 16 - The arrangement of forest types and topography near Fire 41.	55
Figure 17 - The arrangement of forest types and topography near Fire 33.	58

Introduction

Pukaskwa National Park has a mandate to manage the Park to preserve ecosystem integrity. In the boreal forest of Northwestern Ontario, fire is a dominant agent of change. The primary natural cause of forest fire ignitions in natural areas is lightning. An understanding of lightning patterns and the pattern of natural ignitions in the Park area is essential to the management of a natural area subject to natural disturbance.

The Pukaskwa National Park management team is planning to reintroduce fire disturbance to the land (Geomatix, 1996; Heathcott and Crofts, 1997). A spatial and temporal description of lightning strikes would aid in planning this reintroduction.

There are two major questions to be asked. Is there a distinguishable spatial pattern in lightning strikes? Are there any temporal patterns in weather that have influences on lightning ignitions?

Objectives

The goal of the study is to describe lightning strike patterns within Pukaskwa National Park and the surrounding area. The objectives can be identified by the following questions:

- I. Where does lightning strike in Pukaskwa National Park?
 - A. Is the probability of a strike affected by landscape characteristics?
 1. Topography
 2. Land Cover
 3. Ecodistrict
 4. Distance from Lake Superior
- II. When does lightning strike in Pukaskwa National Park? Is there a pattern with respect to Fire Weather Index values?
- III. Which weather characteristics and lightning characteristics lead to lightning-caused fires?

Literature Review

There are several major topics that lead to an understanding of lightning ignitions of fire on forested land. Lightning is a variable phenomenon which routinely occurs in Northwestern Ontario. A detector network routinely records lightning flashes. The manner in which lightning strikes forested land and the probability of ignition of forest fuels is not completely understood.

Lightning

Lightning is a naturally-occurring arc of electricity caused by a difference in charge between two points within the cloud layer, or between a point in the cloud layer and a point on the ground. Lightning in the boreal forest occasionally lights forest fires. The detection of cloud-ground (CG) flashes can help predict forest fire ignitions.

CG flashes can lower positive or negative charge to ground. The majority (90%) lower negative charge. The processes of positive and negative polarity flashes are different, and will be described separately. The following description of lightning is largely derived from Uman and Krider (1989).

Negative CG lightning

The process of a negative cloud-ground flash has several stages. A flash is the total discharge, lowering tens of coulombs (C) of charge to Earth. The typical duration of a flash is up to half a second. A flash has a leader, and one or more high-current pulses called return strokes. The strokes may last 1 milliseconds (ms), separated by several tens of ms.

The first stage in a lightning flash is the development of a stepped leader. The stepped leader is a luminous small body of charge progressing towards the ground in steps of several 10's of meters, at speeds of 2×10^5 m/s. Each step takes 1 microsecond (μ s) to be completed, and the pauses between steps are typically 20-50 μ s. The stepped leader might be carrying 10 C of charge, and have peak currents of 1 kiloampere (kA). The steps of the stepped leader produce forking in the lightning channel.

The potential difference between the stepped leader and the ground is on the order of

10^7 volts (v). As the leader gets close to the ground, a strong electric field is generated at ground level. The electric field is strongest at high points and irregularities on the ground surface. At some point, typically only 10's of metres above the ground, the resistance of the air breaks down, and a discharge moves up from the surface, making contact with the stepped leader. A channel of low electrical resistance between the cloud and the ground is now established, called the lightning channel. Once the channel is established, a return stroke moves up towards the cloud.

The first return stroke typically produces a peak current of 30 kA at the ground, and takes about 100 μ s to reach the cloud. The first return stroke is moving at about 1/3 - 1/2 the speed of light, slowing down as it ascends. The return stroke current drops rapidly to about half of peak value in about 50 μ s. As part of the return stroke, a phase of continued current flow may last into the hundreds of ms. If the return stroke current phase lasts more than 40 ms, then it is termed a long continuing current phase (lcc). It is this first return stroke that is usually detected by the lightning detector system.

A lightning flash may be over after one return stroke, or it may have multiple return strokes. A second stroke may be initiated by a second leader, known as a dart leader, which progresses down the channel opened by the first return stroke towards ground, at about 3×10^6 m/s, lowering perhaps 1 C of charge. If the dart leader jumps out of the channel of the first return stroke, it will become a stepped dart leader. The stepped dart leader is similar to the stepped leader, in that it progresses more slowly, and may branch the channel. Unstepped dart leaders and return strokes after the first return stroke tend not to branch.

Positive CG lightning

Positive flashes generally have the same progression of events as negative lightning flashes, with some notable differences. Positive strikes come from a different layer of the cloud, and represent between 1 and 15% of the total number of strikes in a typical summer thunderstorm (Uman and Krider, 1989).

A positive return stroke typically has a leader which branches less and has much less luminosity. A positive return stroke is more likely to have a long (greater than 40 ms) continuing current phase. A positive flash is less likely to have multiple return strokes.

A positive flash tends to have higher peak currents than a negative flash. Almost all of

the very high-current strikes recorded to structures in several studies were positive strokes (López *et al.*, 1991). Because the positive return stroke may travel at half the speed of the negative return stroke, the strength of a positive return stroke may be underdetected (Mach and Rust, 1993).

Positive return strokes are more likely to have lcc phases than negative return strokes. Between 50 and 100% of positive return strokes have been shown by various authors to have lcc phases (Flannigan and Wotton, 1991), whereas only 25 to 50% of negative return strokes have lcc phases (Uman and Krider, 1989).

Other processes in lightning flashes

Rakov, *et al.* (1994) documented flashes with multiple ground strike points. They determined that about half of the strikes they studied had multiple strike points. Distances between ground positions of the strikes varied between 0.3 and 7.3 km, with a mean of 1.7 km. To measure this, they used a high-speed video camera pointed at a parabolic mirror.

It has been generally accepted that the first return stroke generates the highest currents of the return strokes. This is why lightning detector systems only record the strength of the first return stroke. It has, however, been shown that up to 1/3 of flashes have subsequent return strokes with a higher initial electric field than the first return stroke (Rakov, *et al.*, 1994).

Rakov, *et al.* (1994) also found that lcc's are more likely in subsequent strokes than first return strokes or single stroke strikes. The lcc stroke is often preceded by a high-field stroke and a short inter-stroke interval.

Shindo and Uman (1989) studied a set of 90 strikes near Florida and found that 1 out of 19 of the single stroke CG flashes had an lcc phase, whereas 22 out of 71 of the multiple stroke flashes had lcc phases. They determined that the likelihood of a lcc phase was directly tied to the multiplicity of the strokes.

Summary of the Lightning Process

CG lightning flashes can be of positive or negative polarity. They are initiated by a difference of charge between clouds and the ground.

First, a stepped leader descends. When the stepped leader is close to the ground, charge rises up from the ground. When the two charges meet, a channel of low resistance is formed between the cloud and the ground.

Once the channel is formed, a return stroke goes up the lightning channel. A return stroke typically lasts less than 40 ms. If the stroke lasts longer, it is deemed to have a long continuing current phase (lcc phase).

After the first return stroke, there may be one or more return strokes, initiated by a dart leader. They may also have lcc phases. These subsequent return strokes may or may not follow the same channel as the first.

Lightning-Caused Fire Ignition

The flashes most likely to ignite the forest fuel are those which have a lcc phase (Kourtz and Todd, 1992). Because the lightning detection system in use does not detect lcc phase return strokes, the presence of an lcc phase must be partially inferred from polarity and multiplicity. Flannigan and Wotton (1991) found a link between multiplicity and ignition probability.

The mechanism of lightning-caused forest fire ignition is not known. The presumption has been made that the lightning strikes a particular target because of its conductivity (Kourtz and Todd, 1992). The target conductivity might be affected by moisture content. Short strikes with no continuous current phase do not have enough time to ignite the fuel, although the strike may explode the fuel particle due to steam expansion. The lower, but longer duration, current of the continuous current phase has the time to heat and dry the conductive channel, which increases resistance. The increased resistance increases the amount of heat produced by the electricity passing through, which might then ignite the fuel particle (Kourtz and Todd, 1992).

Lightning Detection Systems

Every flash of lightning produces a burst of electromagnetic energy. This can be observed by turning on a radio during a thunderstorm. Lightning detection systems (LDS's) register the burst of electromagnetic energy and classify it as a CG strike or some other discharge. Lightning detection is a necessary part of fire protection planning. It is to this end that LDS's have been designed. Ontario has a system of detectors across the province, designed by Lightning Location Prediction Incorporated (LLP). Other provinces in Canada and organizations in the United States operate similar systems (Gilbert, *et al.*, 1987; Nimchuk, 1990).

The system in Ontario consists of a network of detectors. The detectors are capable of detecting the electromagnetic burst of a lightning flash. For each flash, the direction can be determined with a precision of approximately 1° (Nimchuk, 1990). The directions and times of flashes are compared by a central computer which calculates a position using triangulation. The system returns a time, position, polarity, strength and multiplicity for each flash. (Noggle, *et al.*, 1976).

In the case of the Ontario network, there are direction finders scattered across the province. The four detectors nearest Pukaskwa National Park are in Geraldton, Hearst, Nipigon and Chapleau (Herodotou, 1990). There are no detectors to the south, which might increase the risk of triangulation errors.

The detector itself consists of a pair of radio antennae capable of detecting electromagnetic bursts from the lightning strike. The centre of the band of detection is near 10 kHz. The burst strength and polarity is detected by an electric field antenna. The azimuth is calculated from a crossed-loop magnetic field antenna (Gilbert, *et al.*, 1987).

The detector is capable of distinguishing between cloud-cloud lightning and cloud-ground lightning. The cloud-ground strike has a large single polarity pulse, while the cloud-cloud flash has a smaller pulse of one polarity followed by the other polarity. Within each cloud-ground flash, there is also a smaller blip in the electromagnetic wave for each return stroke. The detector can detect the return stroke blips and identify return stroke lightning multiplicity (Noggle, *et al.*, 1976).

The detector is limited in range. In British Columbia, lightning events were detected by individual detectors up to 93% of the time at ranges up to 80 km from the detector. The

likelihood of detection was as low as 33%, but was typically between 70% and 80% at this distance, depending on the detector. Low detection probabilities indicated a problem in the system, either in detector location or malfunction. At greater ranges, between 400 and 480 km from the detector, the detection probability dropped to 15%-30%. At the distance range relevant for Pukaskwa National Park, 160 km-240 km, the detector efficiency ranged from 13% to 90%, with a mean of 60% and a standard deviation of 18%. Weak strikes and distant strikes were the least likely to be detected (Gilbert, *et al.*, 1987). An overall detection rate of 70% is typically assumed (Orville and Silver, 1997).

The detection rate of positive polarity strokes may be lower than the rate of negative polarity strokes. Hojo *et al.* (1989) found that 76% of negative first return strokes over the Sea of Japan in summer were detected, while only 69% of positive first-return strokes were detected. The detection efficiency rates are lower in winter.

In Alberta, Nimchuk (1990) found that the precision of the detector system was between 4 and 8 km, but that it went as low as 16 km in the far north of the province. This was attributed to a sparse network of detectors, and an inaccurately reporting detector in the Lesser Slave Lake area. Flannigan and Wotton (1991) assert a similar level of accuracy for the Ontario system, based on the Nimchuk (1990) study.

Passi and Lopez (1989) estimated the errors in direction finder reports caused by features near a direction finder (site errors). After correcting for site errors (up to 9°) using a two-cycle sinusoidal function, they found a randomly distributed error with a mean of 0° and a standard deviation ranging from 0.3° to 0.7°.

The strength report from an individual detector is measured in what are commonly described as “LLP units”. This is an arbitrary scale generated by the detection system, which can be related back to peak currents in amps. The strength reports are then normalized to a range of 100 km. Idone *et al.* (1993) discuss the relationship of these units to the peak current of the individual strokes, under several models of signal attenuation by distance. The most common model is the transmission line model, which estimates signal attenuation based on the assumption that the electrical signals from lightning propagate the way electrical signals propagate down high-voltage transmission lines (Herodotou, 1990).

The reports from the OMNR (1996) report strength on another scale, ranging from 14 to -14. This represents the polarity and relative strength of the signal in a single number.

The polarity of the lightning return stroke may have an effect on the detected strength

of the signal. Mach and Rust (1993) have determined that a positive return stroke carries more current than a negative stroke, by a factor of about four. They comment that values of peak current calculated from the detector network and reported in the literature may be low. This agrees with López, *et al.* (1991), who found reports from a variety of sources regarding strikes to structures and the relative frequency of strong positive strokes.

Herodotou (1990) reports that the strength of strikes in Ontario was being under-predicted by the lightning detection network. The purpose of the study was to estimate the performance of overhead transmission lines in Ontario. The peak stroke current distribution was investigated. The main factors modifying transmission of the signal from source to the lightning detector include signal attenuation over the finitely conducting planetary surface, lightning channel tortuosity (degree of crookedness), and interference from other intermediate electric fields and the ionosphere. The calculations for location and electric field transmissions were also examined. The conclusion that strike strengths are under-reported was based on the transmission line model in use in Ontario and on the lack of certain adjustments in the Ontario system.

Lightning Ignition Prediction

Fire Weather (FWI)

The Canadian Forest Fire Weather Index (FWI) System is the standard system in Canada for measuring the effect of weather on the flammability of forest fuels. It uses weather data to predict the moisture content of several different sizes of wood, and from those moisture content figures, several predictive indices can be generated (Van Wagner, 1987).

The inputs to the FWI system are temperature, relative humidity, wind speed, and 24-hour rainfall. These numbers are measured at noon to predict the fire fuel parameters at 4pm. 4pm is the approximate time on most days when the fuel is going to be at its driest and most flammable. (Van Wagner, 1987)

The Fine Fuel Moisture Code (FFMC) describes the moisture content of the finest fuel

class. These fuels are the litter and other cured fine fuels, generally less than 7 mm in diameter, weighing about 0.25 kg/m², dry weight. This fuel has a time lag to equilibrium moisture content of 2-3 days (Van Wagner, 1987). FFMC is the index that is important to ignition probability (Kourtz and Todd, 1992).

The Duff Moisture code (DMC) describes the moisture content of bulkier fuels - loosely compacted, decomposing organic matter, weighing about 5 kg/m² when dry. The size class of twigs used for this index are the sticks between 7 mm and 50 mm. The DMC responds to changes in weather with a 12 day time lag to equilibrium (Van Wagner, 1987). The DMC can be used to predict fire survival and spread characteristics (Kourtz and Todd, 1992).

The Drought Code (DC) represents the moisture of the deep organic layers and coarse wood with a diameter greater than 50mm, weighing perhaps 25 kg/m² when dry. The time lag to equilibrium moisture content for this fuel type is 52 days (Van Wagner, 1987). The DC is associated with intensity of burn and residence time characteristics of the fire.

The three fuel moisture codes can be combined to produce the Initial Spread Index (ISI), Buildup Index (BUI), and the Fire Weather Index (FWI). These predict, respectively, the rates of fire spread, the amount of fuel available for consumption, and the intensity of the fire (Van Wagner, 1987).

The FWI System has some limitations when used for modelling beyond the original intention of the indices. The indices were originally intended for assessing fire ignition and spread characteristics on a daily basis by using a noon measurement of weather conditions and correlating that with the moisture content conditions at the peak of dryness in the day, typically around 4pm. It does not necessarily follow that the system predicts fuel conditions at any other time of day, or that it takes into account changes in the day's weather that might affect the moisture content of fuels. Heuristic tools have been developed to predict the FFMC variation through the day in fine, settled weather (Lawson, et al., 1996). When the weather changes, as one would expect in weather that produces lightning, the heuristic tools are no longer valid.

The FWI System's applicability to the weather is hampered by the sparse network of weather stations that are the source of weather data. Local point samples of weather conditions may not accurately reflect conditions across broad areas (Kourtz and Todd, 1992). The effect on local weather of individual storm events may be missed by a network of remote weather stations.

Ignitability of Fuels

The two factors that affect the likelihood of ignition and likelihood of continued combustion are moisture content of the organic material and the quantity of flammable material at the site of ignition.

The Duff Moisture Code (DMC) and Fine Fuel Moisture Code (FFMC) have both been found to be significant in the likelihood of ignition of fires from lightning. In Ontario in 1988, Flannigan and Wotton (1991) found the DMC to be the most significant weather variable for prediction of ignition and survival to discovery. Nash and Johnson (1996) found FFMC to be more significant in Alberta and British Columbia over four fire seasons.

The character of fuels at the site of ignition affects the flammability of the site. The vegetation complex at a site has a very strong effect on fire ignition and behaviour. The structure of the stand, the surface fuel type, forest floor type and ladder fuel quantity all affect fires. These are variable at a local scale, but can be represented by an idealized fuel array, such as that used by Forestry Canada (1992) in the Fire Behaviour Prediction (FBP) system.

The organic content of the soil, specifically the duff layer, is a significant factor in the soil flammability. Soils with a low organic content are less flammable than soils with a high organic content (Frandsen, 1987). This can affect the survival of fires to detection.

Lightning Weather Patterns

The large-scale weather patterns associated with dry fuels and high likelihood of lightning are high pressure systems, especially those systems that are persistent for long periods of time. A high pressure system brings warm, dry, clear weather to an area. This results in the drying of the fuel matrix. Street and Alexander (1980) have shown that all five of the large fires in the Pukaskwa area from 1931 to 1956 were preceded by high-pressure systems. This is in agreement with other studies: "high pressure systems result in the co-occurrence of drier fuels and higher strike densities than during other synoptic weather conditions" (Nash and Johnson, 1996, p.1860).

Atmospheric instability can also be associated with higher lightning densities. Turbulence associated with atmospheric mixing leads to the development of thunderstorms

and their associated lightning. A typical pattern is that the ground-level air layer is heated by the sun during the afternoons of hot, sunny summer days. The instability of cool, dense air above warm, light air causes convective cells, which can generate the tall cumulo-nimbus clouds of local thunderstorms. The lightning strike density varies with the number of these convective cells and the height of the tops of the clouds (Nash and Johnson, 1996).

Within the Pukaskwa National Park area, there is a local factor that affects thunderstorm activity patterns. Lake Superior has an influence on the frequency of clear weather, and on the convective activity that causes storm development and therefore lightning activity (Pers. Comm., Crofts, 1998).

Analysis of Lightning Data

Analysis of lightning data can be classified into two major groups: probability of strike analysis, and analysis of weather conditions that lead to ignitions from lightning.

Van Wagendonk (1991) analysed the spatial distribution of lightning strikes at Yosemite National Park in Wyoming and found that topography, especially elevation, has a substantial effect on lightning strike distribution. Strikes are more likely at higher elevations, but aspect and slope are not significant. Because vegetation in Yosemite is primarily controlled by elevation, the differentiation of lightning strikes by vegetation type was similar to the differentiation by elevation.

Nash and Johnson (1996) considered fire ignitions in Alberta and British Columbia and found that the probability of ignition was very low for any given lightning strike. Strikes that ignited a fire could be differentiated by vegetation cover type, and by atmospheric pressure at the time of the strike. High atmospheric stability decreased the likelihood of precipitation and the likelihood of high ISI values. The important FWI components for ignition and detection of a fire were FFMC and to a lesser extent DMC.

Flannigan and Wotton (1991) studied ignitions in 1988 in the western part of Northwestern Ontario, in UTM zone 15, roughly west of Upsala. They found that stroke multiplicity and DMC were the most important factors in ignitions, although they could only explain 47% of the variance of ignition probability per day.

Lightning strike density and distribution

Since the development of the lightning strike detection system, there have been several studies of the distribution of strikes, both spatial and by strike characteristics. Strike density has been studied in the United States (Orville, 1994; Orville and Silver, 1997), the Sea of Japan (Hojo, *et al.*, 1989), Australia (Petersen and Rutledge, 1992), and Norway (Huse and Olsen, 1984).

Orville and Silver (1997) describe lightning strike density in the contiguous United States from 1992-95, and Orville (1994) describes the same for the years 1989-91. They found a range of strike densities from 0 to 13 CG flashes per square kilometer. Notably, the south shore of Lake Superior is in an area of low CG strike density, in all years. The rate of CG strikes along the south shore is consistently below 1.0 strike/km². The range of CG strike numbers across the country ranges from below 0.5 strikes/km² to 13 strikes/km² per year, assuming that 70% of strikes were detected.

Probability Density Estimation

The kernel technique is a non-parametric approach to estimating the density of a population of locations from a sample of the locations. This method was summarized and described effectively by Silverman (1986; Worton, 1989; Wand and Jones, 1995). The kernel method involves summing a “kernel” function applied to all point locations from the sample. A typical kernel function is a normal curve, but other functions can be used where appropriate. A smoothing factor is usually applied to make the resulting density estimations more closely resemble the presumed population from which the sample is derived. The smoothing factor is either chosen from a subjective examination, or from an automatic error-minimization technique.

Kernel estimators have well-understood properties that have been investigated extensively in the statistical literature (Worton, 1989). They were initially described by Rosenblatt (1956). Epanechnikov (1969) described an alternate kernel function to the gaussian normal function in order to speed up calculations.

A kernel estimator can be described as a sum of “bumps”. The multivariate kernel density estimator is defined at any point \mathbf{x} as

$$\hat{f}(\mathbf{x}) = \frac{1}{nh^d} \sum_{i=1}^n K \left\{ \frac{1}{h}(\mathbf{x} - \mathbf{X}_i) \right\} \quad \text{Equation 1}$$

where \mathbf{K} is the kernel function, \mathbf{h} is the smoothing factor, d is the dimensionality, and \mathbf{X}_i is the location of any of the sample points that represent the function. The function is evaluated for a point \mathbf{x} . The calculation is usually performed repeatedly for multiple points in a regular sequence to represent a curve or surface (Silverman, 1986).

The kernel function \mathbf{K} is a radially symmetric unimodal probability density function, like the standard multivariate normal density function:

$$K(\mathbf{x}) = (2\pi)^{-d/2} \exp(-\frac{1}{2}\mathbf{x}^T\mathbf{x}) \quad \text{Equation 2}$$

$\mathbf{x}^T\mathbf{x}$ in Equation 2 is the matrix transpose of the point \mathbf{x} , multiplied by the point \mathbf{x} . The product of \mathbf{x} and the matrix transpose of \mathbf{x} , in the two-dimensional case, is

$$\mathbf{x}^T\mathbf{x} = \mathbf{x}1 * \mathbf{x}1 + \mathbf{x}2 * \mathbf{x}2, \quad \text{Equation 3}$$

or the squared euclidean distance. \mathbf{x} in the Equation 2 is equal to the contents of the curly braces in the Equation 1 (Silverman, 1986). This particular kernel function is also called the gaussian kernel. Other kernel functions can be used.

To visualize a kernel estimator, imagine a univariate case, with 7 data points (\mathbf{x}), as in Figure 1(a). A standard normal curve for the kernel function and a smoothing parameter (\mathbf{h}) of 0.4 units is shown in Figure 1(b). Figure 1(c) shows kernel functions superimposed over each of the data points. Figure 1(d) shows $\hat{f}(\mathbf{x})$, the kernel estimate of the distribution from which the seven points were drawn. The estimate suggests that the density is higher in the middle, with one main peak, but that there are relatively wide “shoulders” to the curve (Silverman, 1986).

The smoothing parameter (\mathbf{h}) is the most significant parameter to the estimation of densities using the kernel method. The smoothing parameter could be described as the width of the individual kernels. The appropriate choice of smoothing parameter can show the maximum amount of information available without introducing too much spurious detail to the estimate. Figure 2 shows three choices of smoothing parameter applied to the data from Figure 1. Figure 2(a) shows an oversmoothed estimate, with all detail smoothed away.

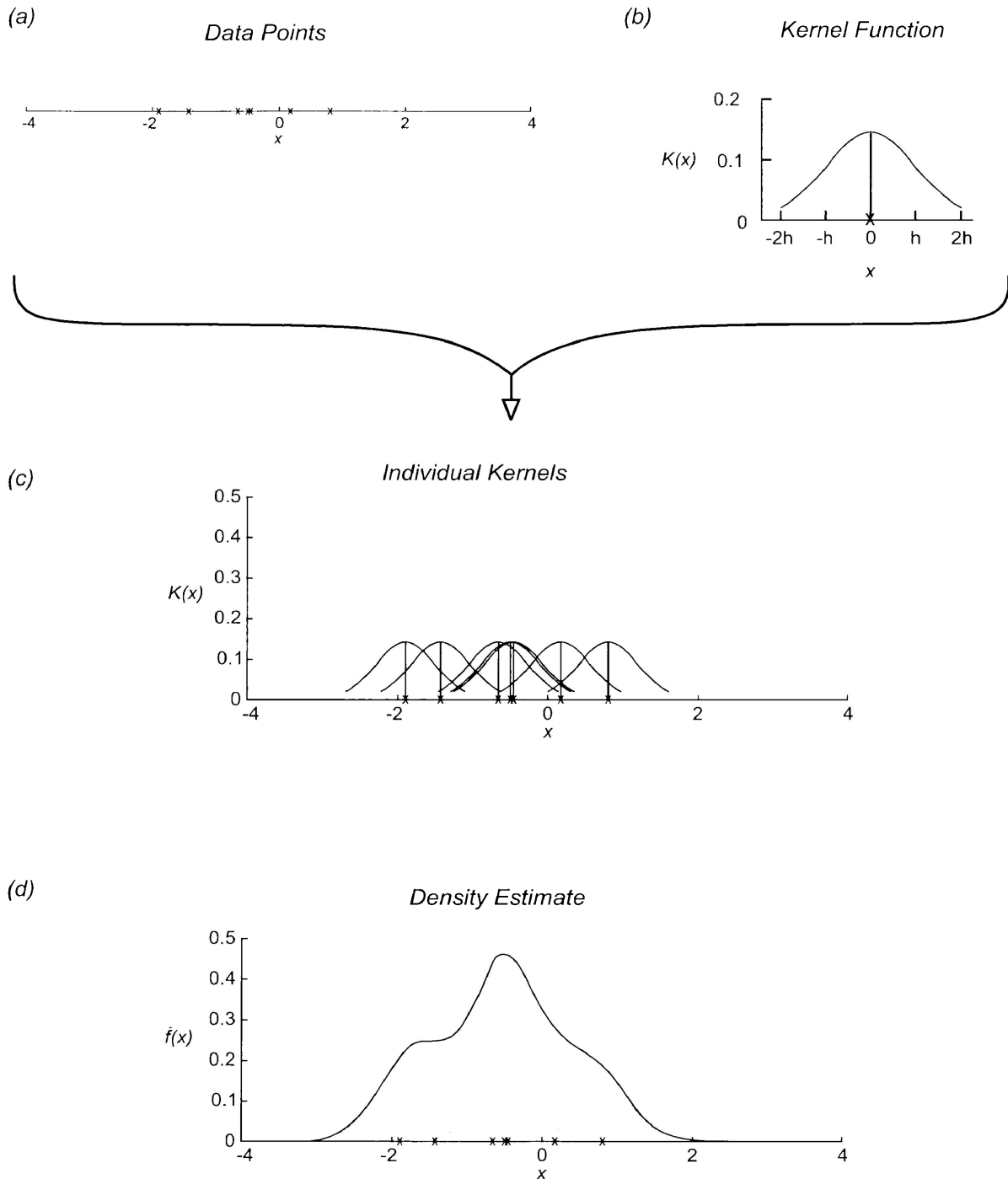


Figure 1 - Schematic diagram of kernel estimator process. In step (a), data points are gathered. In step (b), the kernel function and smoothing parameter (h) are chosen. In this case, the kernel function is the normal curve, and the smoothing parameter is 0.4 units. In (c), the kernel function has been calculated for each data point. In (d) the individual point kernels from step (c), here in grey, have been summed to produce an estimate of the density of data points (black).

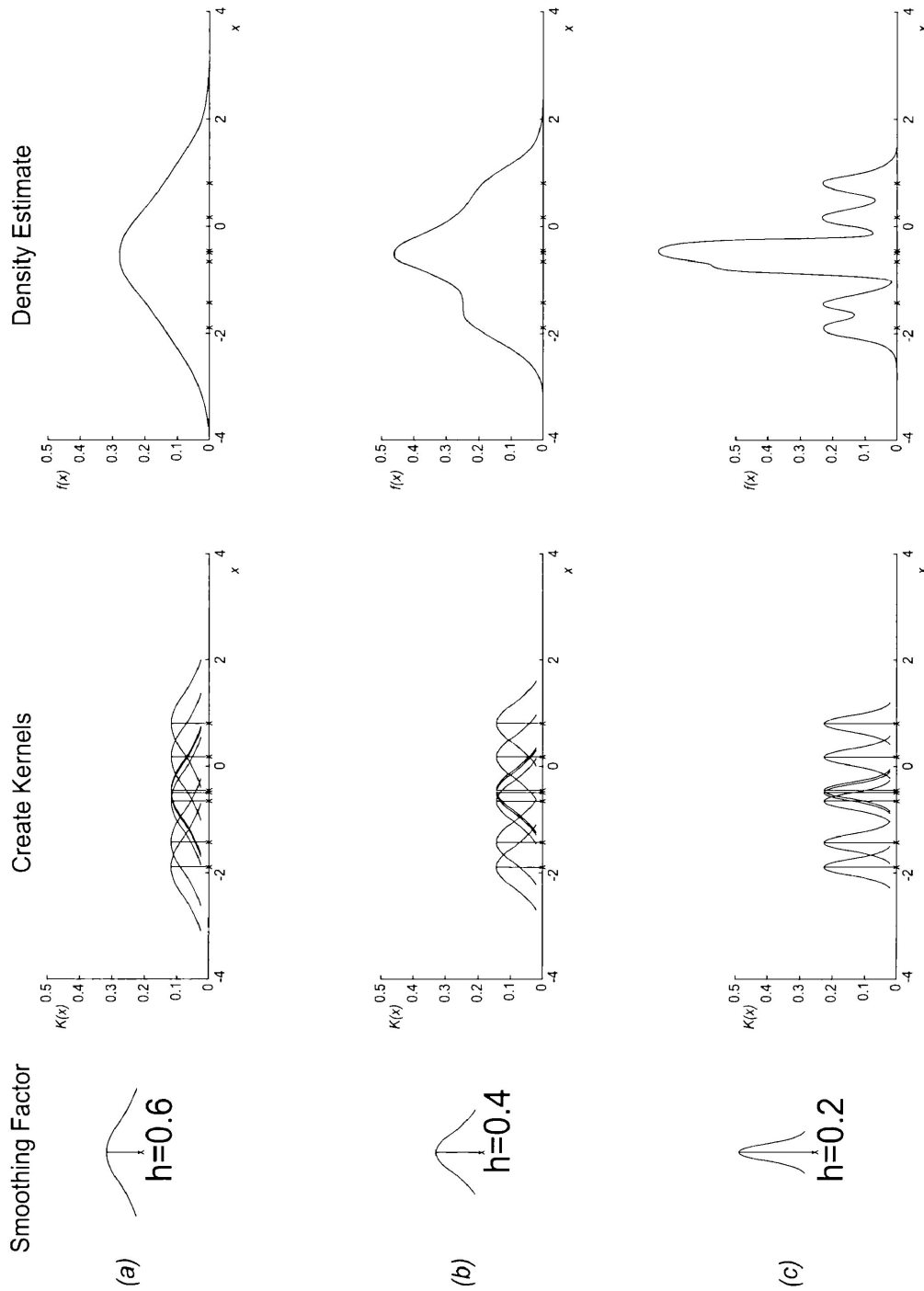


Figure 2 - The effect of smoothing parameter choice on density estimates. The data in each example are the data from Figure 1. Density estimate (a) is likely oversmoothed, as it is showing the data to be fairly unimodal, and has smoothed away all the detail within the data. (b) is probably adequately smoothed and shows some detail in the distribution. The “shoulder” in the left side of (b) suggests a slight multimodality in the data. (c) shows a jagged, dramatically undersmoothed estimate of density.

Figure 2(b) shows an adequately smoothed estimate, with some of the detail internal to the data visible- it has “shoulders”. Figure 2(c) shows spurious detail, and is undersmoothed.

The same can be seen with many more samples. Figure 3 shows three estimates of a known distribution, each derived from a set of points. In this case, the original distribution is expressed by the equation

$$f_1(x) = \frac{3}{4}\phi(x) + \frac{1}{4}\phi_{1/3}(x - \frac{3}{2}). \quad \text{Equation 4}$$

1000 samples were taken from the distribution, and used to estimate that distribution. The dashed line indicates the original distribution, while the solid line indicates an estimate of the distribution. Kernel estimator (a) is undersmoothed, and is showing spurious detail. Estimator (b) is oversmoothed, showing a lack of detail by ignoring the thin peak to the right. Estimator (c) shows a much closer estimate of the original distribution (Wand and Jones, 1995).

The smoothing factor in a two-dimensional case is properly expressed with two separate smoothing factors, one in each of the axes. This makes cross-comparison of analyses difficult. Instead, what is commonly done is a transformation of the data to an arbitrary coordinate system by dividing each coordinate by a vector made up of the standard deviations of the axes (Seaman and Powell, 1997), or transforming one axis to have the same variance as the other (Kenward and Hodder, 1996). This allows a single smoothing parameter to be chosen that reflects reasonably closely the separate smoothing factors for each axis.

Smoothing factors are typically expressed either as a raw number from the coordinate axes of the system, or as a fraction of h_{ref} (Kenward and Hodder, 1996; Seaman and Powell, 1997). h_{ref} is derived from the equation

$$h_{ref} = n^{1/6} \sqrt{(\sigma_x^2 + \sigma_y^2)/2}, \quad \text{Equation 5}$$

in the two-dimensional case, where s^2 is the sample variance in either of the two dimensions. The use of h_{ref} is useful when the coordinate axes are to be transformed, and when attempting to use a similar smoothing factor with different point distributions.

In some cases, it may be appropriate to apply a variable smoothing factor to the kernel function. This can be done to weight the tails of the distribution, or to weight the cores of the distribution (Kenward and Hodder, 1996; Silverman, 1986). In the analyses where a variable smoothing factor is applied, it is termed an “adaptive” approach to smoothing, as opposed to a “fixed” approach. The adaptive approach smoothes the function more in areas of lower density, and smoothes less in areas of higher density. This can lead to fewer extraneous

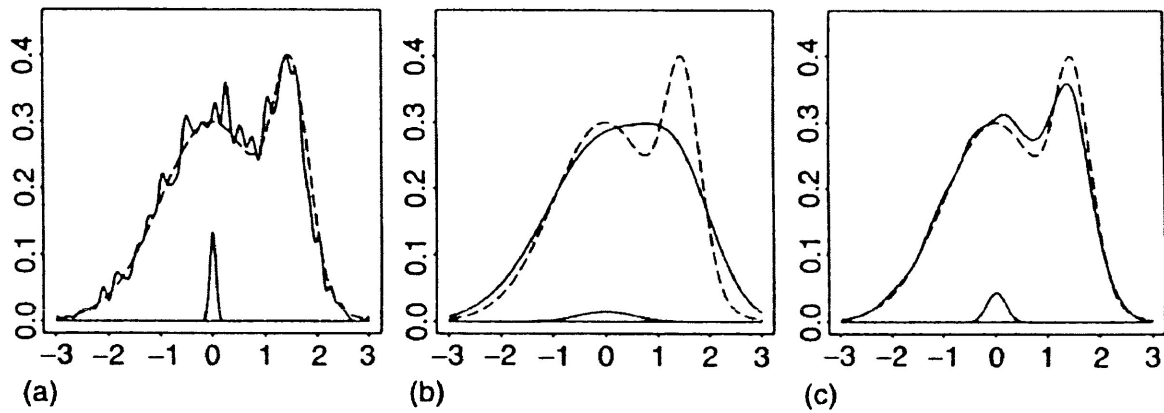
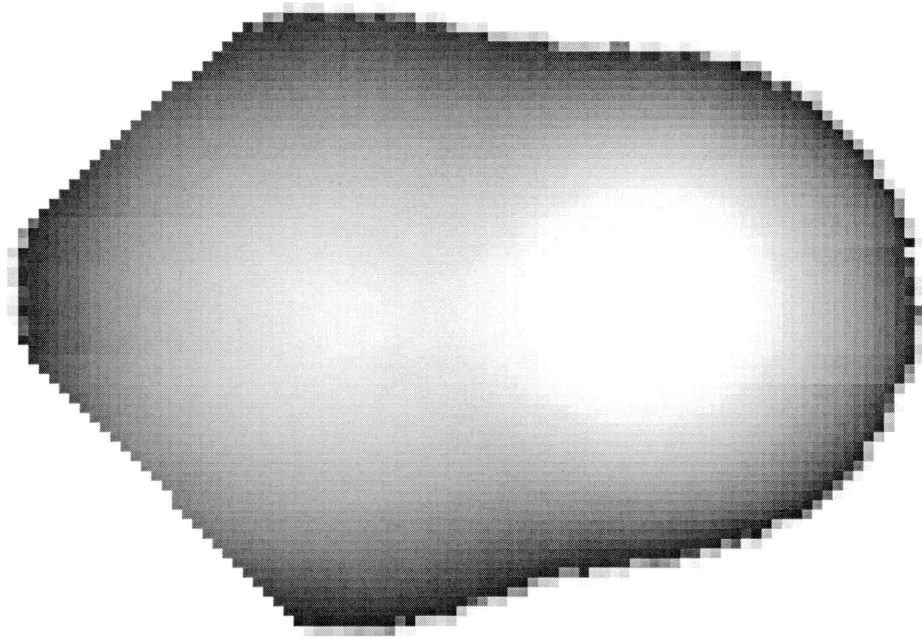


Figure 3 - Three kernel estimators of a known distribution, using 1000 samples from the distribution described in the text (Equation 4). The dashed line shows the original distribution. The solid line indicates an estimate. The smoothing parameters are (a) $h=0.06$, (b) $h=0.54$, and (c) $h=0.18$. In the center bottom of each diagram is a depiction of the kernel function being used for the estimate. (a) is undersmoothed, and shows spurious detail. (b) is oversmoothed, and has ignored real detail. (c) is properly smoothed. Diagram from Wand and Jones (1995).

(a)



(b)

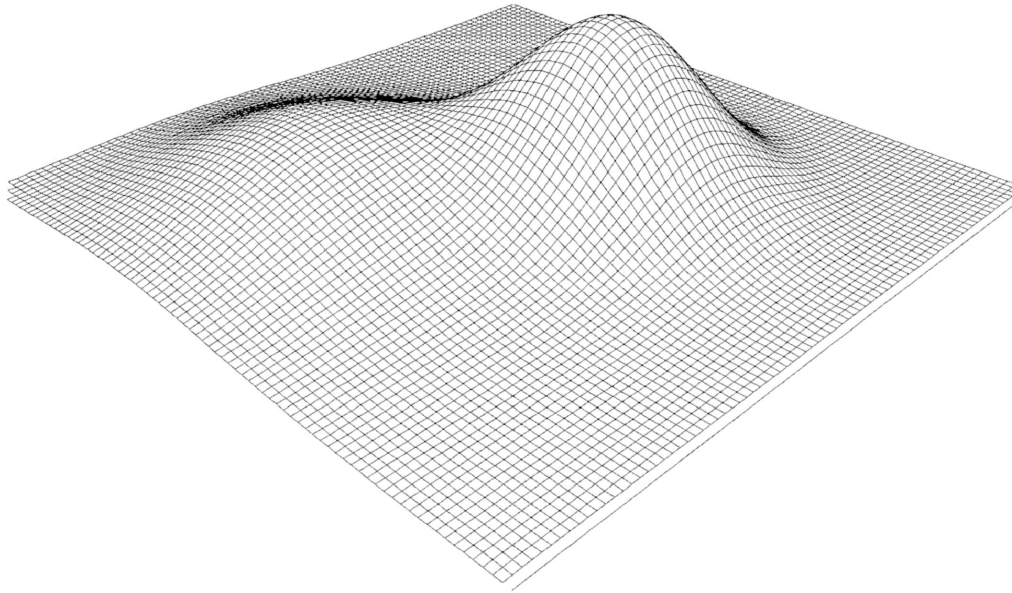


Figure 4 - Simulated bivariate probability density field, in two dimensions. The probability field is derived from a sum of two normal curves. (a) shows a orthographic (map) view, using brightness to indicate increasing density. (b) shows a simulated perspective view of the same field.

“bumps” in the tails of the distribution, while preserving interesting structure in the core of the distribution.

A density estimation procedure produces an empirical estimate in the form of a list of probabilities for each coordinate in the sample space. In one dimension, a line is produced, as in Figures 1, 2, and 3. In two dimensions, a raster cell map of the sample coordinate space is typically produced. Each square in the “graph paper” represents a probability. Figure 4 shows an example of this, represented in two ways. The field shown in Figure 4 is derived from the sum of two bivariate normal curves. Figure 4 (a) shows a orthographic view - a sheet of graph paper - with shades of grey representing the density. Figure 4 (b) shows a perspective view of the same simulated density field.

The result of the point density estimation is typically a raster cell map containing probabilities that a new point would be in that cell. This method of expressing the densities produces the volume under the surface at any given point for a cell of a specific size. The sum of all the cells should be precisely one (1). If it is not one, then there is a substantial systematic error.

The areas of current research concerning kernel methods are clustered into two main groups- applications of kernel methods, and automatic smoothing parameter choice procedures.

The kernel method of density estimation is used widely. It can be used for curve-fitting in situations where a parametric solution is inappropriate, particularly due to multimodality or discontinuity in the distribution. It is used in wildlife research for habitat utilization and home range studies (Lawson and Rodgers, 1997), where the animals use many small areas, progressing across the landscape. It has been used for estimating probabilities for a discriminant analysis, for estimating hazard rates, non-linear data dimensionality reduction, and in cluster analysis (Silverman, 1986).

The smoothing parameter can be chosen manually, from knowledge of the system being investigated and from experience with the data. This can be time-consuming and is inappropriate for large data sets, or for large collections of data sets. Manual selection of smoothing parameter is also not very reproducible, especially not by people inexperienced in the technique. For these reasons, automatic smoothing parameter selection techniques are being developed. These methods use the data to estimate a pilot estimate, from which an estimate of error can be derived. The most appropriate smoothing parameter is that which

minimizes the error function. The most common method of automatic smoothing parameter choice is a least-squares cross-validation. Newer methods include “solve-the-equation plug-in” methods and smoothed bootstrap methods (Jones, *et al.*, 1996).

Setting

Pukaskwa National Park is located on the north shore of Lake Superior, in Ontario, Canada. Figure 5 shows the Park in relation to the surrounding area. It also shows the location of notable places within the Park.

Marathon is the nearest town to the Park, located to the north of the park. Other relatively large towns nearby are White River, to the northeast and Wawa, to the southeast. All of these towns are on or near Highway 17. The Park can be reached from Highway 17 using Highway 627 from the north. This is the only highway access to the Park.

The Park Office is located at Hattie Cove, at the north of the Park. Immediately near the office is a weather station. There are two other weather stations, at Soldier Mountain and at Otter Cove.

Two other locations which are used in this study are the mouth of the Pukaskwa River and Widgeon Lake. These two locations, with Hattie Cove are used as an expression of the spatial extent of the Park.

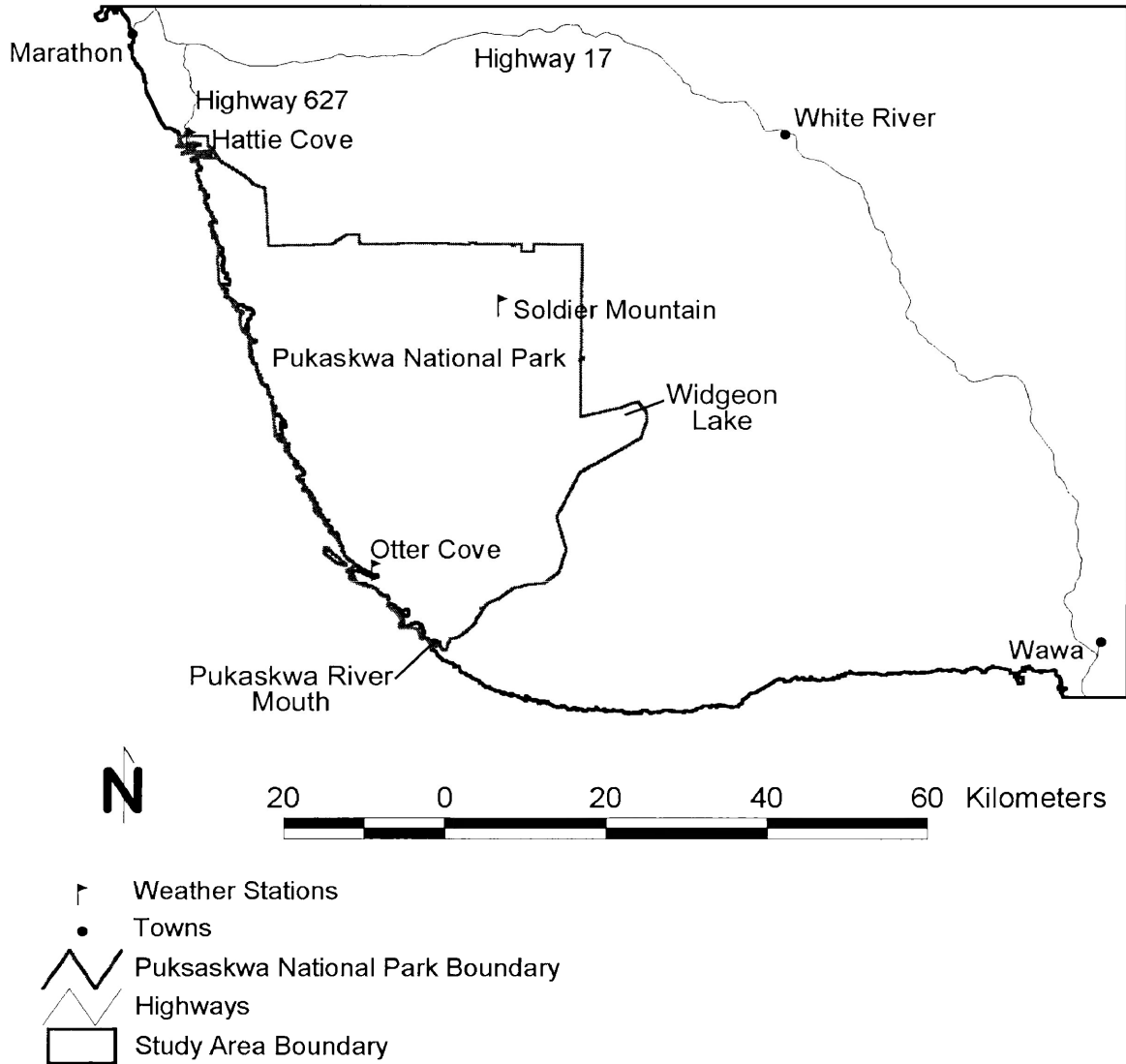


Figure 5 - Local Setting of Pukaskwa National Park. The Park is located on the North Shore of Lake Superior.

Data Sources

Pukaskwa National Park has provided data on climate, ignitions, and vegetation. The Ontario Ministry of Natural Resources (OMNR) has provided the lightning strike data. Barometric pressure data were obtained from the United States National Oceanographic and Aeronautics Administration (NOAA).

Data were collected and processed using a geographic information system (GIS), and a database program. The vegetation, ecodistrict, topographical and proximity to Lake Superior data were all maintained in a raster format. This format can be likened to a piece of graph paper, with a value for each square. The individual squares are known as pixels, which have a resolution (linear dimension of a side) and an area. All other data were maintained as discrete locations or records in a database.

Lightning Detection System Data

The information from the lightning detection system (LDS) consists of records of each CG flash, or strike. For each strike, the time and date, latitude, longitude, polarity and strength of strike are recorded. The multiplicity, or number of return strokes, is not reported, although the system is capable of reporting it (Noggle, *et al.*, 1976).

Information for the greater Pukaskwa area was made available by the OMNR for the last three years. Data were requested for the area between 47° and 49°N and 84.5° and 86.5°W, which covers the Park and the area between Highway 17 and Lake Superior from Marathon to Wawa.

The locations of the LDS direction finders is published, for example, in Herodotou (1990). The geographic locations of the towns in which the direction finders are located and distances from chosen locations was determined from the Natural Resources Canada (1998) Geographic Names Database.

Weather

Weather information obtained from Pukaskwa National Park consists of the records from stations within the Park. The information for 1994-1996 is being used because the automated weather stations inside the Park were set up in 1994. The hourly temperature, relative humidity and precipitation are recorded at these stations. The stations are distributed around the park, at Hattie Cove, Soldier Mountain, and Otter Cove (Figure 5).

Weather data was present for all three stations, but there were some periods where data was not collected, or was unusable. The entire season's weather records for 1994 at Hattie Cove was not available because of problems associated with the data. At Hattie Cove, the fire seasons started on May 5, 1995 and April 1, 1996. At Otter Cove, the seasons started June 3, 1994, May 11, 1995, and June 6, 1996. Data collection for the 1995 season at Otter Cove was cut short July 26. At Soldier Mountain, the season start dates were June 3, 1994, May 5, 1995, and June 6, 1996. The fire season extends into October.

Barometric pressure data have been obtained for Wawa airport from the National Climatic Data Center (NCDC) in the United States. The "Pukaskwa" weather station listed in the station listings was not reporting for part of the period of interest, so Wawa Airport data were used. The data were provided to the NCDC by the Atmospheric Environment Service, Environment Canada.

Ignition Locations and Times

Forest fire ignitions within the Park are routinely recorded by the Park. Only two fires have occurred in the three years under consideration. The fire reports were made available by Pukaskwa National Park (OMNR, 1995a and OMNR, 1995b).

Vegetation Coverage

Vegetation coverage for this study will be derived from previously classified satellite imagery captured in 1994 and in 1991 (Pukaskwa National Park, 1995). Land cover classes in this study are derived from that classification. The classes are described in Table 1. The vegetation coverage is at a resolution of 18 m, for a pixel area of 325 m².

Table 1: Vegetation classification system from a classification of satellite imagery of Pukaskwa National Park and area. Satellite imagery was from the Landsat Thematic Mapper in 1991 and 1994.

Class	Description	Abbreviation
1	Conifer > 80%, 76-100% Crown Closure	Con8>76C
2	Conifer > 80%, 51-75% Crown Closure	Con8>51C
3	Conifer > 70%, 25-50% Crown Closure	Con8>25C
4	Deciduous > 80%, 51-100% Crown Closure	Dec8>51C
5	Mixed Conifer >50%, 25-50% Crown Closure	Mcon525C
6	Mixed Deciduous >50%, 25-50% Crown Closure	Mdec525C
7	Non-Productive	Nonprod
8	Inert: rock, poorly vegetated	Inert
9	Water	water
10	Depleted Lands, <4 years old	dep<4
11	Depleted Lands, >4 years old	dep>4
12	Roads, <4 years old	roads<4
13	Roads, >4 years old	roads>4
14	Railway Line	railline
15	Ontario Hydro Transmission Line	hydro
16	Urban	urban
17	Cloud	cloud

Topographical Information

Topography was derived from Ontario Base Map (OBM) data for the area. A raster surface interpolated from the point data from the OBM series was processed to provide elevation values, and peak elevation values. Both elevation and topographic position have been suggested as reasonable factors to investigate for influence on lightning strike density. The raster surface was previously prepared with a square resolution of 100 m, using inverse distance weighting of 12 points per pixel with the GRASS 4.15 program `r.surf.idw` (USA-CERL, 1995). Each pixel in the topographical coverage is 1 ha.

Ecodistrict Information

Ecodistricts are complexes of relatively homogeneous topography and vegetation. An ecodistrict coverage was supplied by Pukaskwa National Park. There are five ecodistricts within the Park. This information was supplied at a resolution of 288 m, with a cell area of 8.3 ha. A map of the 5 ecodistricts is shown in Figure 6.

Distance from Lake Superior Data

The data describing the distance of each pixel from the shoreline of Lake Superior were prepared from the the vegetation coverage. A contiguity analysis was performed on the water component of the vegetation data. Lake Superior was identified as the biggest contiguous piece of water, and was extracted as a new data layer. The new Lake Superior coverage was buffered by twenty kilometer intervals. There were six classes of distance within the extents of the vegetation data layer. This data layer was prepared at a resolution of 407 m, or 16.6 ha/pixel.

Data Coverage

The areas of coverage of the various sets of data in this project are shown in Figure 7. The geographic extents of the individual data layers do not match. The analyses were performed using the smallest relevant areal extent from the data. Results were adjusted accordingly.

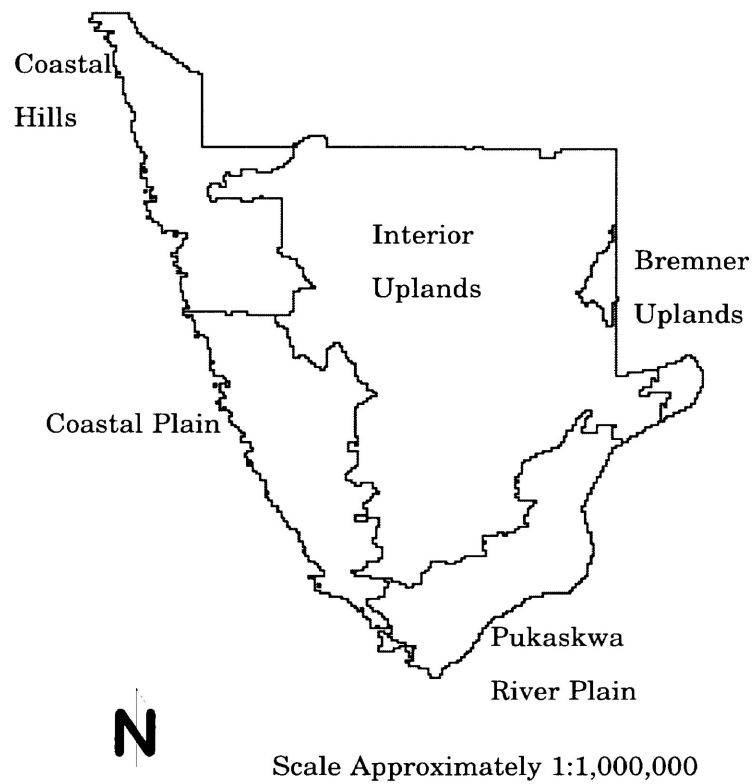


Figure 6 - The five ecodistricts of Pukaskwa National Park, supplied by the Park. An ecodistrict represents a landscape-level homogenous collection of topography, landform and vegetation types.

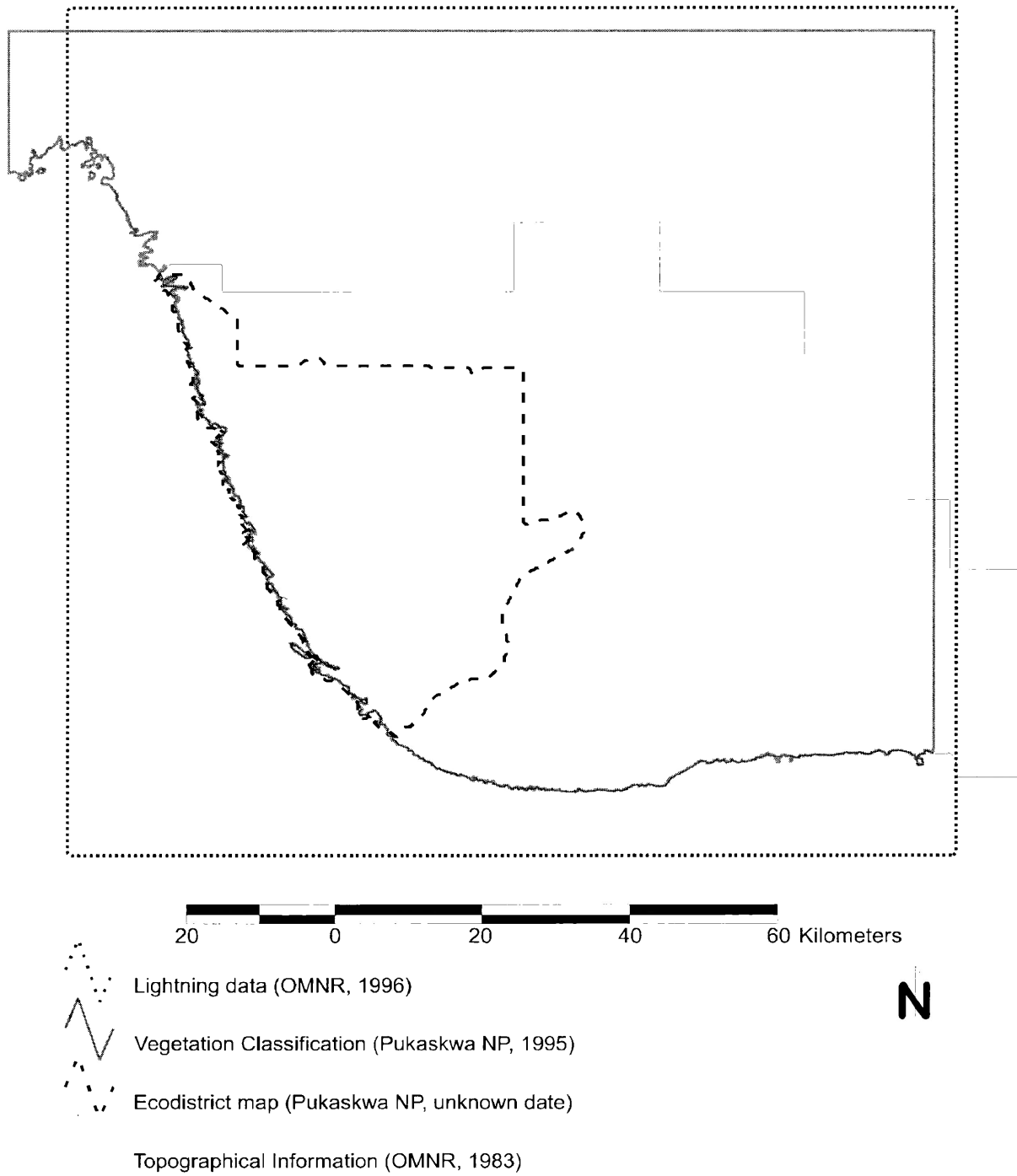


Figure 7 - Areal extents of individual data sets used in this project.

Methods

This study consists of three major components, related to the three identified objectives. The first section is an analysis of lightning probability density cross-tabulated with landscape characteristics. The second section is a probability density analysis of the weather measurements at the time of a strike record. The third section is a summary of conditions at the time of fire ignitions in the Park.

The data were viewed in a variety of ways to look for interesting patterns in the data. Histograms were used as a viewing tool, where appropriate, and simple database queries were used to increase personal familiarity with the data. Overlay of the data layers in a GIS showed the location of data in relation to other data.

Section 1 - Where?

Lightning strike probability was predicted for all parts of the Park from three years of lightning strike records. The average probability generated from that procedure was calculated for each class of vegetation, each class of topography, each class of ecodistrict, and each of several bands of distance from Lake Superior. The statistical significance of each mean was then calculated.

Data Preparation

Two probability density maps were generated, one using only the positive polarity strikes, and the other using all strike records. The positive polarity strikes are assumed to be more significant, because they may have a higher likelihood of igniting fires.

The probability density maps were generated using a fixed kernel method, with a gaussian kernel. The smoothing factor was calculated from the specification of 1° error at the direction finders (DF's), and the approximate distance from the three nearest DF's to three corners of the Park, at Hattie Cove, Pukaskwa River mouth, and Widgeon Lake.

The smoothing factor was chosen to be equal to

$$h = \frac{\sum_j \sum_i [\tan(1^\circ) * D_{ij}]}{ij} \quad \text{Equation 6}$$

where i is the number of DF's being considered (three) and j is the number of points for which this calculation is being performed. The distances (D_{ij}) were calculated at the three corners of the Park, at Hattie Cove, Pukaskwa River mouth, and Widgeon Lake to the nearest three detectors to those points. The smoothing factor was rounded to the nearest 500 m. A simplified diagram of this calculation is shown in Figure 8.

Two topographic class maps were generated from the topography map provided by the Park. The first map was a level slice of the continuous topography into 7 equal elevation divisions, ranging from 183-642 m. The second topographic map was a map of local high points. This map was generated by applying a round maximum filter with a radius of 1 km. Points that were the same height as the product of the maximum filter were identified using map algebra. These points were the highest point within a kilometer.

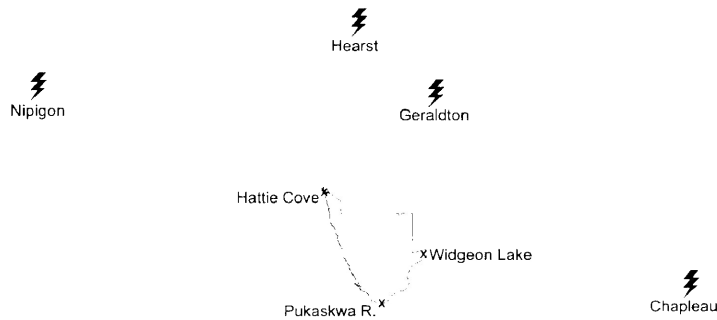
Analysis

The probability density maps were cross-tabulated with the vegetation classification, the ecodistrict map, the topographic class maps, and the distance from Lake Superior map. The resolution of the analysis was set to be that of the class map, with the probability density map resampled to match it. The mean of the probability density map within each class was calculated.

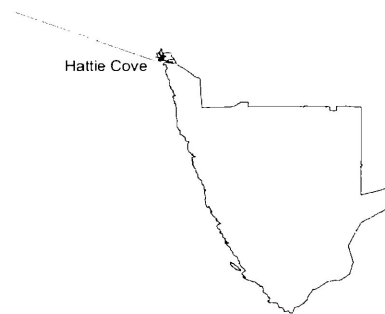
Because the spatial extents of the various class maps were different from each other, the probability density maps had to be adjusted to represent the restricted area of the class map. Probability density was summed over the area of the class map. The probability density maps were multiplied by the reciprocal of this sum. After this procedure, the restricted area probability density maps retained the characteristics of probability density maps, in that the volume under the surface was one.

The probability density means are not specifically informative without an idea of the statistical significance of the mean. Each class probability density (PD) mean was compared against the range of variability in values calculated in the same way, but derived from random sets of points, instead of points selected by a factor of interest (like ecodistrict).

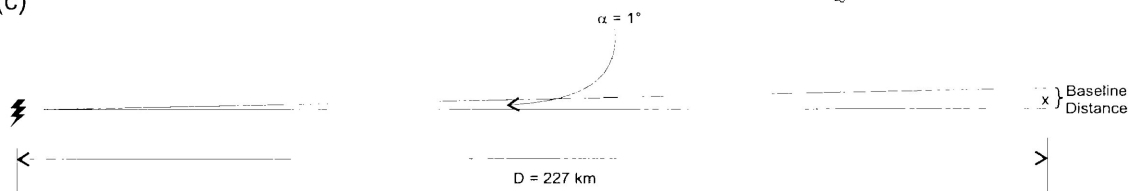
(a) All Direction Finders and Park Corners



(b) An Example: Hattie Cove Corner of Park, Nipigon Direction Finder



(c)



Using Trigonometry:

$$\text{Baseline Distance} = \tan(\alpha) * D$$

Figure 8 - Simplified description of how the smoothing factor was calculated for the preparation of the lightning density maps. This is a schematic only. (a) There are four Direction Finders (DFs) near Pukaskwa National Park. (b) For each combination of DF and corner of the Park, there is a Baseline Distance, which is a description of the specifications of error of the DFs at that distance. The example shown is the Baseline Distance for the Nipigon DF and Hattie Cove. (c) The calculation of the Baseline Distance involves trigonometry. In the example, Nipigon is 227 km from Hattie Cove, so $D=227$ km. The error specification for the DFs is 1° , so the angle $\alpha=1^\circ$. Calculating through the formula in (c), the Baseline Distance is 4.0 km. The smoothing factor for the kernel analysis is the mean of the nine Baseline Distances (Only considering the three nearest any Park corner), rounded to the nearest 500 m.

The range of variability in PD means was calculated for a class by calculating PD means for each of 500 random sets of points. The random sets each had as many pixels as the class of interest. From the 500 random-set PD means, a general mean was calculated. The deviations of the random-set PD means from this general mean describe the range of variability that we can expect from a random selection of points. The percentage of random-set PD mean deviates that are greater than the class-of-interest PD mean deviate (p value) describes the probability that the class of interest is not a statistically significant factor. The p value answers the question “Did this factor affect the probability density surface?”

A class mean was considered to be statistically significant if less than 5% of the random sets of points had a probability density mean with a deviation from the overall mean greater than the class of interest deviation. This can be expressed as a p value less than 0.05. This follows the logic of the analysis of variance (ANOVA), as discussed by Brown (1995).

Section 2 - When?

Weather measurements were compared with lightning strike times to give a picture of when lightning strikes. Daily Fire Weather Index (FWI) values were used as the coordinate system assigned to each lightning strike record. A probability density map was developed, based on the FWI coordinate system.

Daily FWI values were calculated using methods from Van Wagner (1987), for each of the three weather stations at the Park- Hattie Cove, Soldier Mountain, and Otter Cove. The start dates of the fire season were derived from snow depth data, according to Van Wagner (1987). Starting values for the FWI calculations were drawn from the data files provided by the Park. These calculations were done at the Park using WeatherPro (Remsoft, 1996).

The probability density surfaces for this section of the analysis were prepared in a coordinate system using Fine Fuel Moisture Code (FFMC) and Duff Moisture Code (DMC) values as the axes. Of FWI indices, these two indices are the most closely associated with fire ignition.

Probability density surfaces in the FFMC-DMC coordinate system were developed from the lightning strike records and the daily weather records from all three weather stations.

Surfaces were calculated from the daily weather at all stations of each year, at each weather station for all years, and from the weather on the day of each lightning strike.

The adaptive kernel method was used to calculate the probability density surfaces. A smoothing factor was chosen by subjective evaluation, after standardizing the coordinates to make the variance in the two axes identical. The subjective evaluation was performed by repeatedly calculating probability density surfaces with a range of smoothing factors. The probability density surface with the best compromise between spurious detail (undersmoothing) and lack of detail (oversmoothing) was selected.

The weather on the day of a lightning strike was determined by matching the dates in the lightning and weather files. Only lightning strike records for days with valid FWI codes were included in this analysis. The lightning strike records could then be plotted in the FFMC-DMC coordinate system instead of in a geographic coordinate system.

Section 3 - Fires

Each of the two fires that occurred in the study period has been described by tabulating the fire report data, the vegetation and topography data for the immediate vicinity, and the weather conditions at the time of the fire and for some time before and after. All of the data that were made available have been included.

Software

The software used for these analyses was from one of two sources, either from the GRASS GIS, version 4.2 (Baylor University, 1997), or written expressly for the purpose. GRASS was used to coordinate the data, project the data into a common coordinate system, provide storage, compare the data, and display data.

The kernel procedures used for this analysis are derived from Tufto (1994). He follows the methods of Worton (1989), which are based on Silverman (1986). The code provided was originally used to discuss the effect of “discretization”- the inaccuracy of measurement - on the estimates of sizes of animal home ranges. The source code provided by Tufto was limited to 300 observations, so it was necessary to modify it. Extensive tests were made to ensure

that the results produced by this program were correct. Modifications were necessary to allow a link to GRASS data structures, and to allow certain improvements to be made, including the coordinate transformation process. The program was compiled under GNU C, v.2.7.2.2 (FSF, 1997).

Results

The lightning strike information consists of a point location, a time, and a strength/polarity rating for each ground strike. Notably, none of the strike records indicated return strokes. The strikes are mainly negative polarity- seven percent of the strikes records were positive polarity. There were 8666 strikes recorded in locations not in Lake Superior and within the area under study in the years 1994-1996.

There were 1248 strikes recorded within the Park boundaries in the three-year period. The mean number of strikes per square km is 0.38, assuming a 60% detector efficiency. This is consistent with Orville (1994) and Orville and Silver (1997) on the south shore of Lake Superior. This represents 14% of the strikes in about 20% of the area. The study area as a whole had 0.58 strikes/km², assuming the same 60% detector efficiency.

The majority of strikes records were between -4 and -10 strength. There was a mirror-image distribution of positive and negative polarity strikes, except for the difference of the number of strikes. The distribution of strikes is shown in Figure 9.

There was a significant difference between the number of strikes with a numerically even score and the number of strikes with a numerically odd score. A X^2 test comparing the count of odd strikes and even strikes against half the count of strikes shows ($X^2=113$, $df=1$, $p=0.000$) that the even and odd counts are not the same. There were significantly more odd strikes than even strikes.

Section 1 - Where?

Probability Density Maps

The lightning strike probability maps were calculated using a fixed kernel method from the lightning strike record locations. Two maps were prepared, one for the positive strikes only, and one for all strikes. These two maps are presented in Figures 10 and 11. The distribution of values in the probability density maps is non-normal, and resembles a Poisson distribution.

Some variation in the density of strikes can be seen even in Figures 10 and 11. A visual comparison between the area north of the Park and the centre of the Park reveals that there is a higher density of strikes north of the Park than in the Park. The same can be seen

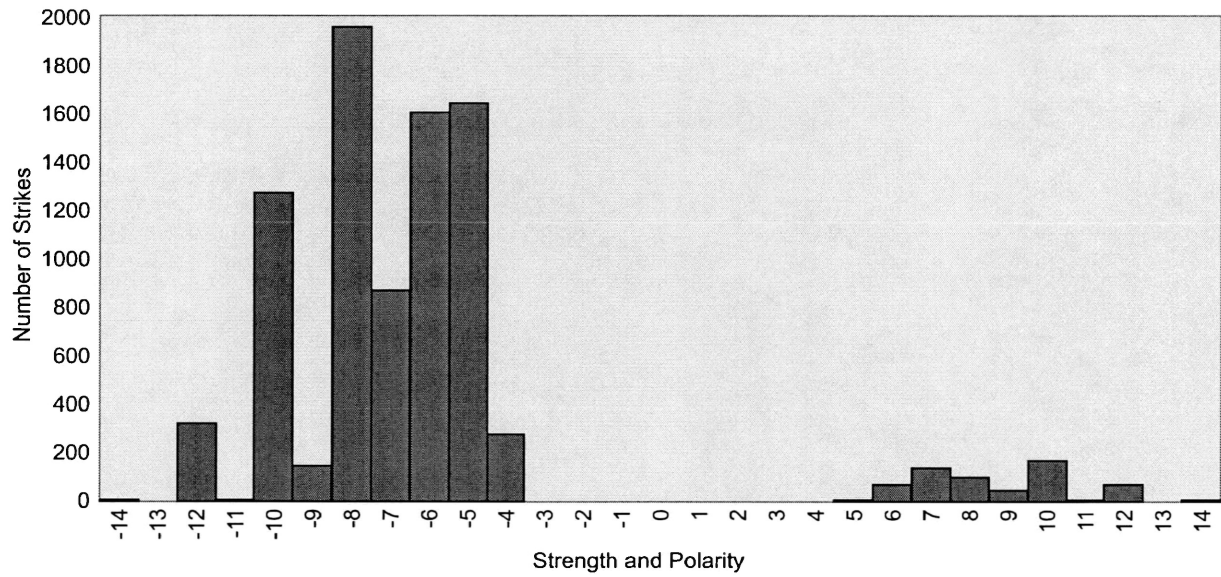


Figure 9 - Distribution of strikes by strength and polarity scores.

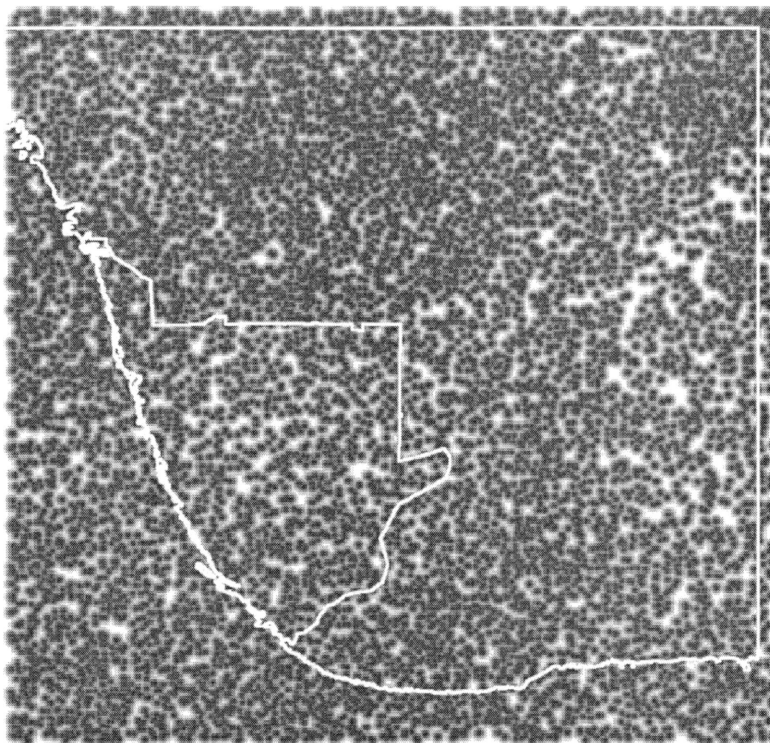


Figure 10 - Probability density map of all lightning strikes. The values in the map represent the relative likelihood of a strike having happening in that area in the study period. Increasing probability is indicated by an increased intensity of black.



Figure 11 - Probability density map of positive polarity lightning strikes. The values in the map represent the relative likelihood of a strike having happening in that area in the study period. Increasing probability is indicated by an increased intensity of black.

southeast of the Park. Within the Park, there is still some variability. The centre of the Park can be seen as an area of lower strike density than the north or south extremes of the Park.

The smoothing factor was calculated to be 3.5 km. This was calculated based on the distances presented in Table 2. The mean baseline distance, rounded to the nearest 500 m, is 3.5 km.

Throughout this section, in the text and in tables, mean probabilities are stated. These probabilities are stated in probability per pixel. The size of the pixels varies with each analysis.

Topographic Class Maps

The level-slice of the elevation map was prepared by dividing the range of elevations into 7, and calculating the new class of each pixel by which range of elevation it fell into. The results of this calculation are shown in Figure 12.

The map of local peaks was prepared by applying a round maximum filter to the elevation map to make a map of the height of the highest point within two km, then using map algebra to identify locations whose elevation was the same as in the resultant map. The results of this are shown in Figure 13.

Crosstabulations

The crosstabulations of the probability density maps with topographic class produced two tables of mean probabilities, and their standard deviations. These are shown in Table 3.

It can be seen from Table 3 that lower elevation locations seem to be more likely to get struck by lightning than higher elevations, contrary to intuition. This is not a consequence of there being more low elevation locations than high elevation locations. A location in the lowest elevation class is 2.9 times more likely to get struck by lightning than a location in the highest elevation range, at least for all strikes. All of the means for all strikes were significantly deviant from random.

For positive strikes, a similar pattern can be seen, although the highest probabilities seem to lie in the middle elevations, with lower elevations not far behind. A location in the

Table 2 - Table of distances to lightning detection system direction finders (DFs) to the three corners of Pukaskwa National Park, at Hattie Cove, Widgeon Lake, and Pukaskwa River mouth. DFs are at Geraldton, Hearst, Nipigon and Chapleau. The tangent of 1° multiplied by the distances are also shown.

Name	----- Distances (km) -----			----- Baseline Distance (km) -----		
	Hattie Cove	Pukaskwa R	Widgeon L	Hattie Cove	Pukaskwa R	Widgeon L
Chapleau	226	247	209	3.9	4.3	3.6
Geraldton	136	207	192	2.4	3.6	3.4
Hearst	157	212	220	2.7	3.7	3.8
Nipigon	227	183	165	4.0	3.2	2.9

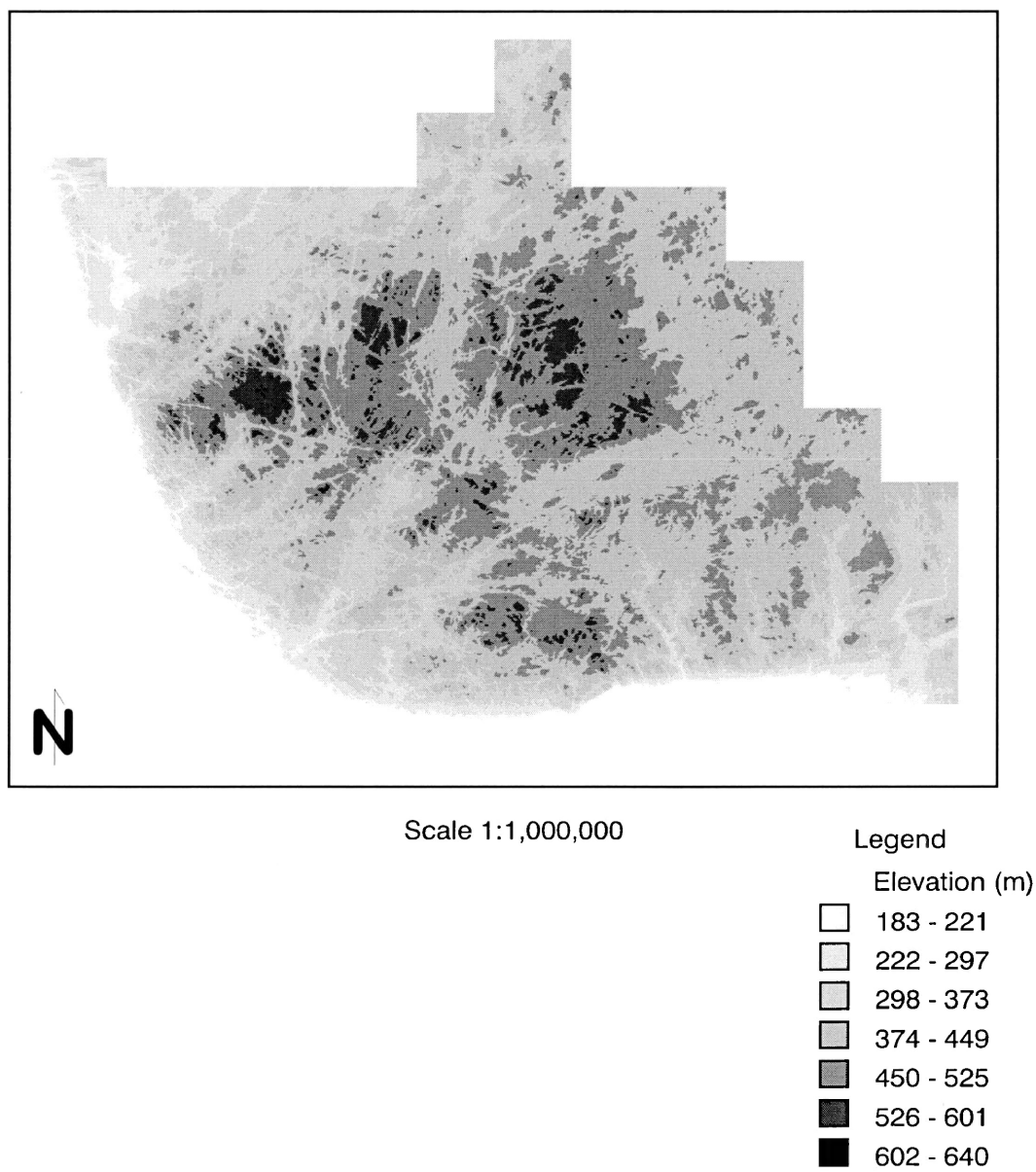


Figure 12 - Elevation map converted into 7 elevation classes of equal width.

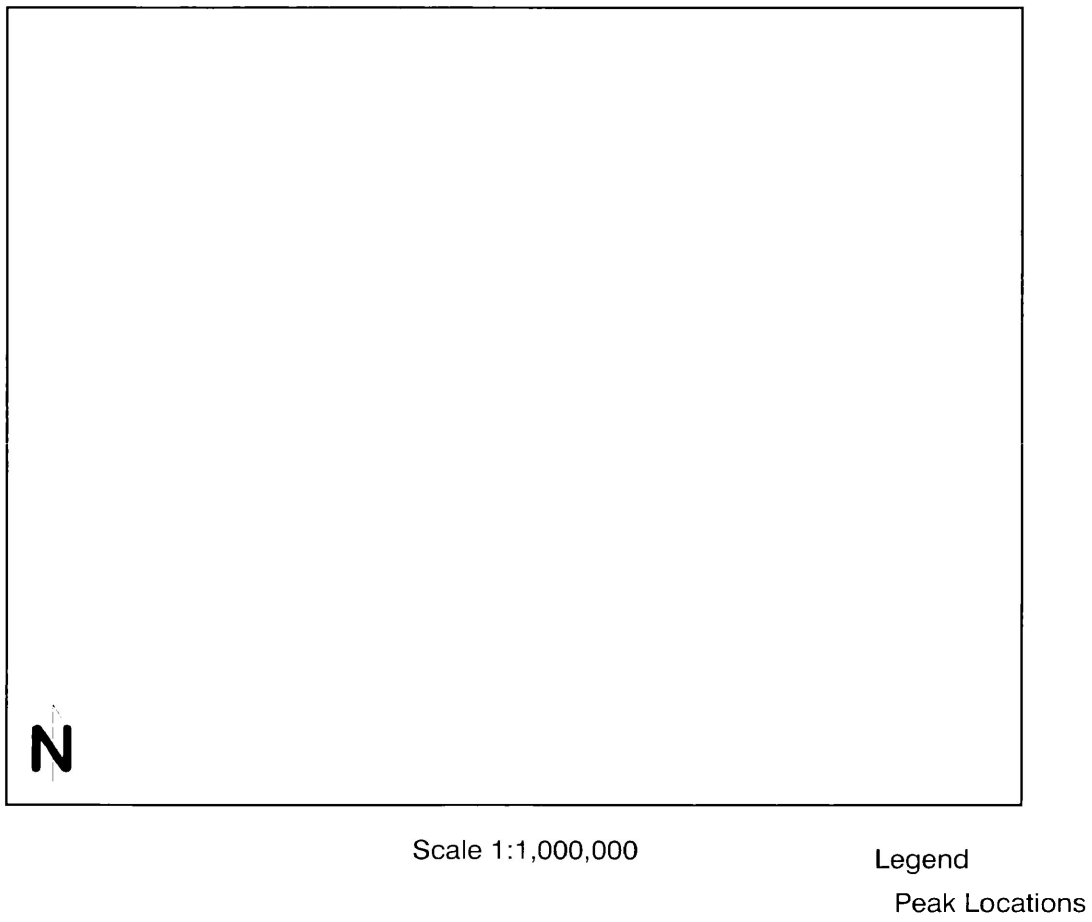


Figure 13 - Peak elevation map derived from the elevation map using a maximum filter and map algebra.

Table 3 - Crosstabulation of the probability density maps with topographic class maps for both all strikes and positive strikes.

Elevation Category	-----All Strikes -----		-----Positive Strikes ----	
	Mean	p	Mean	p
183 thru 221	1.88E-06	0.00	1.72E-06	0.00
222 thru 297	1.84E-06	0.00	1.76E-06	0.00
298 thru 373	1.72E-06	0.00	1.83E-06	0.00
374 thru 449	1.48E-06	0.00	1.39E-06	0.00
450 thru 525	1.49E-06	0.00	1.49E-06	0.06
526 thru 601	1.17E-06	0.00	1.19E-06	0.00
602 thru 640	6.53E-07	0.01	1.13E-08	0.11

298-373 m class is 160 times more likely to get struck by a positive strike than a location in the top elevation class. The highest elevation class did not have a statistically significant mean, however. The greatest difference between significant means was between the same middle class and the second-highest elevation class, 526-601 m, where there was a factor of 1.5 difference.

Locations in the top elevation class (602-640 m) are much less likely to get struck by positive polarity strikes than locations in all the other elevation classes. The class stands alone, at less than 1% of the probability of the class next below it. This is probably an artifact of the process, given the number of positive strikes, and the significance of the results. It should be presumed that this effect does exist, given that the same effect (at a lower level) can be seen in the analysis of all the strikes.

The general pattern that can be observed in both the all-strike analysis and the positive strike analysis is that the mean probability of strikes drops from a high at the lowest elevations to a low at the highest elevations. There is deviation from this pattern in the all-strike analysis, but it is not a large deviation. The deviation that can be seen in the positive strike analysis is larger, and can be seen to be marginally within the range of random variability. This pattern is highly counter-intuitive, as we generally expect higher elevations to be areas of higher lightning activity.

The crosstabulations of the probability density maps with peak class produced two sets of mean probabilities, and their statistical significances. These are shown in Table 4.

The results reported in Table 4 support the intuitively reasonable suggestion that peaks get hit by lightning more than other areas. The probability of a peak location getting struck by lightning is 1.2 times higher than the rest of the population of locations in the area for which topography is available. The probability of a peak location getting struck by a positive strike is 2.0 times higher than that of a non-peak location. These results are all significantly different from random.

The crosstabulation of vegetation class by probability density values (Table 5) showed that a typical location has a probability of between 3.2×10^{-8} and 3.5×10^{-8} of being struck by lightning. Exceptions to this are the Inert class (Rock, poorly Vegetated), recently depleted lands, the rail line and urban areas, all of which show a higher probability of being struck. The Inert class is obviously higher, at 6.3×10^{-8} . The Inert class shows an opposite response for positive strikes, with a much lower probability of being struck than the common

Table 4 - Crosstabulation of the probability density maps with peak class maps for both all strikes and positive strikes.

Elevation Category	-----All Strikes -----		-----Positive Strikes ----	
	Mean	p	Mean	p
Peak	1.83E-06	0.03	3.06E-06	0.00
Not Peak	1.55E-06	0.03	1.54E-06	0.01

Table 5 - Crosstabulation of the probability density maps with the vegetation class map for both all strikes and positive strikes.

Category	----- All Strikes -----		----- Positive Strikes ----	
	Mean	p	Mean	p
Conifer>80% 76-100% Crwn Clos.	3.31E-08	0.02	3.29E-08	0.02
Conifer>80% 51-75% Crwn Clos.	3.36E-08	0.02	3.62E-08	0.00
Conifer>70% 25-50% Crwn Clos.	3.52E-08	0.00	3.96E-08	0.00
Decid>80% 51-100% Crwn Clos.	3.08E-08	0.00	3.04E-08	0.00
MixedConifer>50% 25-50% Crown	3.28E-08	0.57	3.11E-08	0.00
MixDecid>50% 25-50% Crown Clos	3.18E-08	0.00	3.46E-08	0.00
Non-Productive	3.36E-08	0.02	2.97E-08	0.00
Inert: rock poorly vegetated	6.28E-08	0.00	1.52E-09	0.00
Depleted Lands <4 years old	4.05E-08	0.00	3.06E-08	0.00
Depleted Lands >4 years old	2.99E-08	0.00	2.08E-08	0.00
Roads <4 years old	3.91E-08	0.00	4.28E-08	0.00
Roads >4 years old	3.42E-08	0.12	3.44E-08	0.13
Railway line	4.24E-08	0.00	2.11E-08	0.00
Hydro	3.87E-08	0.00	3.92E-08	0.00
Urban	5.05E-08	0.00	3.50E-08	0.24
Cloud	3.90E-08	0.00	2.88E-08	0.00

probability range of other classes. Almost all of these results must be assumed to be statistically significant from random, with the exception of a mixed woods class with greater than 50% Conifer, and older roads for the all-strike analysis and older roads and urban classes for the positive-strike analysis.

It is notable that the conifer classes all have a higher probability of getting struck by any strike than the deciduous classes. The same can be said for the positive strike analysis when only the unmixed stands are considered.

Another set of classes that shows an interesting high probability of strikes is the human-dominated classes, which mostly show a high probability. This can be seen in the recent depleted lands, recent roads, railway, hydro corridor, and urban classes for the all-strike analysis. This same picture is not as clear for the positive strike analysis, but the trend is there. The reason for this is not immediately clear.

Ecodistricts near the Lake Superior coastline have a higher mean probability of getting struck by lightning than interior ecodistricts (Table 6). The largest significant difference was between the Pukaskwa River Plain, at 5.92×10^{-5} and the Interior Uplands, at 4.15×10^{-5} . The Coastal Hills were more likely to be hit by a positive strike than other ecodistricts, especially the Bremner Uplands, although all of the positive results are within the bounds of random variation.

The combination of elevation results and ecodistrict results suggest that the most noticeable effect on lightning density was one of distance from Lake Superior. The analysis of distance from Lake Superior showed a pattern where the likelihood of a strike was higher at the shoreline and lower inland, until 80 km from the shore, at which point, the values rose again (Table 7). This area is to the Northeast of Pukaskwa National Park, past the town of White River.

The results of the positive strike analysis show different zones of high activity than the analysis for all strikes. There is a higher probability at the shoreline and an even higher probability just inland (21-40 km). Between 41 and 100km, there is a lower probability of a strike, with another high at the extreme distance. Presumably the increased probability of strikes at such distance from Lake Superior is not associated with Lake Superior directly, but rather some other local factor.

Table 6 - Crosstabulation of the probability density maps with the ecodistrict class map for both all strikes and positive strikes.

Category	----- All Strikes -----		----- Positive Strikes -----	
	Mean	p	Mean	p
Coastal Hills	4.72E-05	0.59	5.71E-05	0.88
Interior Uplands	4.15E-05	0.00	4.48E-05	0.15
Coastal Plain	5.33E-05	0.00	4.99E-05	0.25
Pukaskwa River Plain	5.92E-05	0.00	3.28E-05	0.09
Bremner Uplands	3.99E-05	0.29	1.91E-05	0.83

Table 7 - Crosstabulation of the probability density maps with the map of distance from Lake Superior for both all strikes and positive strikes.

Distance (km)	----- All Strikes -----		----- Positive Strikes -----	
	Mean	p	Mean	p
0-20	1.57E-05	0.01	1.59E-05	0.01
21-40	1.54E-05	0.01	1.78E-05	0.01
41-60	1.60E-05	0.01	1.31E-05	0.01
61-80	1.43E-05	0.01	1.52E-05	0.01
81-100	1.81E-05	0.01	1.33E-05	0.01
100+	2.63E-05	0.01	3.93E-05	0.01

Section 2 - When?

The data for this analysis were the weather observations and the lightning strike dates. Density estimates of weather during lightning and of daily weather conditions were generated for comparison. The results of the analysis can suggest how patterns of weather and patterns of lightning coincide.

Daily Weather Probability Density

A density surface describing the patterns of weather through the season was derived for each year at all weather stations, and for each weather stations in all years. These density surfaces are in a coordinate system using the FFMC and DMC as axes.

The smoothing factor for this procedure was chosen to show reasonable detail, while not providing too much detail. A range of smoothing factors was tested, from $0.1 h_{ref}$ to $1 h_{ref}$. This range showed undersmoothed surfaces and oversmoothed surfaces. A reasonable compromise seemed to be $0.3 h_{ref}$. The same smoothing factor was used throughout all the analyses to simplify calculation and improve comparability for similar diagrams.

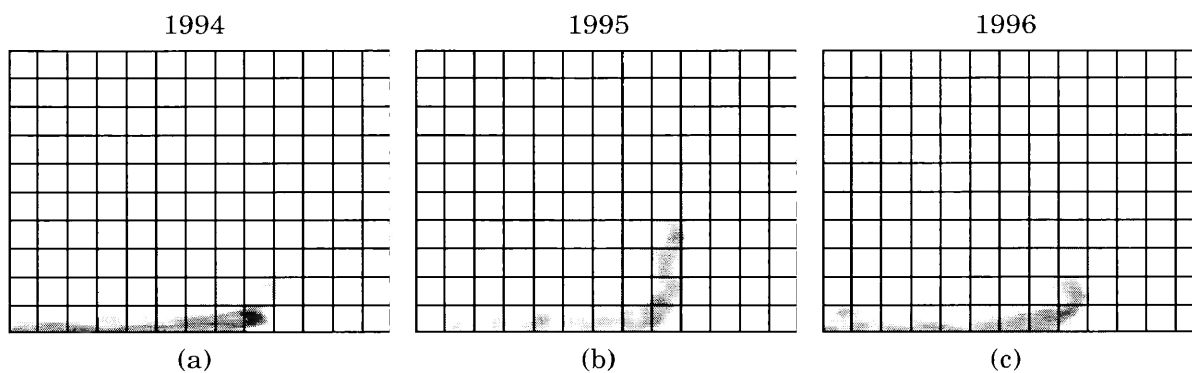
Days By Year

The analysis of daily weather in each of the three years showed that the three years had different weather, but that there was some commonality in the shape of the distributions. The pattern that can be seen in Figure 14 (a), (b), and (c) is an “L” shaped distribution. There are many days with a low DMC and a range of FFMC. There are some days with a high FFMC and a range of DMC. In (b), there are many days with a high FFMC and a medium-high DMC. The results suggest that there are many days that are effectively unsuitable for fire survival, but that there are some days that have high index values.

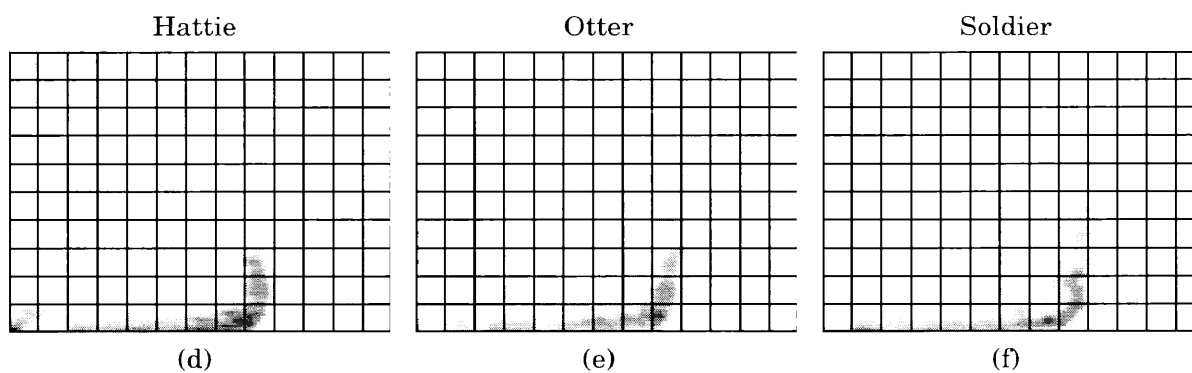
In some years, there is a higher proportion of high-risk fire weather than other years. The order of “seasonal severity” is 1995, 1996, 1994. The fire season in 1995 was the most fire-prone, at least with respect to weather, of the three. The 1994 distribution of days is weighted to moderate FFMC and low DMC values (Figure 14 (a)). The 1995 season has a significant weighting of high FFMC and high DMC days (Figure 14 (b)). The 1996 season was intermediate (Figure 14 (c)).

The similarity of pattern between years is not surprising. The weather in the Pukaskwa

Days by year, All weather stations



Days by weather station, All Years



Lightning strikes by nearest weather station, All Years

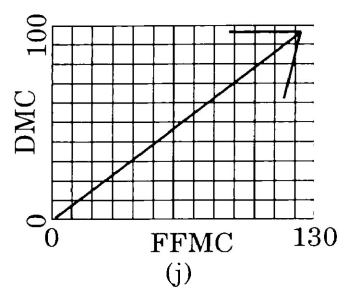
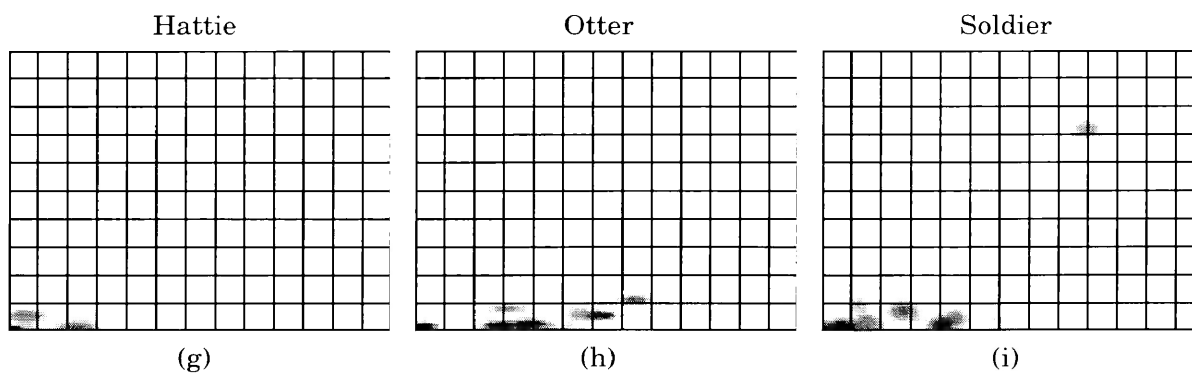


Figure 14 - Probability density surfaces in the FFMC-DMC coordinate system. Graphs (a) to (f) are derived from the weather on individual days through three seasons at three weather stations. Graphs (g) to (i) are derived from the weather codes on the day of individual lightning strikes, by closest weather station. (j) shows the axes for all graphs. Each square in all the graphs represents 10 units of the axis. Fire risk increases non-linearly with the arrow in (j).

area is generally considered to be cool and wet compared to other areas away from Lake Superior. This would suggest that we should expect mainly cool, wet weather, with occasional sunny breaks. The difference in weighting of the pattern between years is also not surprising. Fire seasons are expected to vary in severity.

Days By Station

The pattern of weather that can be observed at the three weather stations over the three year period is essentially similar to the pattern observed in the year-specific analysis. The same days, split up in a different way, show a similar general pattern. In this analysis, the three stations can be rated for severity of fire weather. The Hattie weather station shows the least fire-inducing weather (Figure 14 (d)), while Otter Cove weather station shows the highest DMC codes at the top end of FFMC (Figure 14 (e)). Soldier Mountain falls between them (Figure 14 (f)). This pattern of “station severity” is somewhat surprising, given that the Soldier Mountain station is significantly inland from the Lake, while the other two are coastal. The dissimilarity between Hattie Cove and Otter Cove weather stations is interesting.

Lightning Weather Density

Each strike record was matched to the FWI codes for that day at the nearest station using the date. Density surfaces were calculated for the three weather stations using the FFMC-DMC coordinate space. The smoothing factor was chosen in the same way as it was in the daily weather analysis, and $0.3 h_{ref}$ was chosen.

The common pattern shown between the stations is that most strikes happen at low values of DMC (Figure 14 (g), (h) and (i)). The range of FFMC at which lightning occurs varies between stations. This fits a picture of most storms having significant rainfall, or happening as part of a system of cloudy, cool weather. Each storm event seems to cause its own node of density in the surface.

There is a significant group of lightning strikes near Soldier Mountain weather station. This particular set of strikes happened on June 24, 1995, with FFMC values of 89.6 and DMC values of 72.0. The storm happened after 10pm. The following day, the indices were

62.2 and 50.9, respectively. By then, the storm was over. This was the only large, concentrated group of strikes that happened at high values of DMC and FFMC. This storm event stands alone as the only significant group of strikes in highly flammable fuel conditions.

Section 3 - Fires

In the three-year period under examination, there were two fires ignited by lightning in the Park. They are reported as Fire 33/95 and Fire 41/95. Both fires were detected in the north part of the Park, on June 24th and 25th, 1995. They were both extinguished in short order, at small sizes.

In the days leading up to the fire ignitions, the weather was warm with a consistently high barometric pressure. On the 25th of June the wind was high and from the east, the temperature was near 20°C and the relative humidity was high. 4.2 mm of rain fell in the 24 hours up to noon on June 25th. Over the next few days, during the fire-fighting effort, the temperature remained moderate and the relative humidity rose (Table 8). On the 27th of June, another 26.2 mm of rain fell. There was a weak high pressure system in the area for the entire period of both fires, until the fires were under control, after which the pressure dropped (NCDC, 1997).

The locations of the two fires are shown on a map in Figure 15. This map shows the fires in relation to the Park boundary.

Fire 41

Fire 41 was near UTM coordinates 590500, 5365500. It was first reported June 25 at 14:30. By the time it was first attacked at 15:40 the same day, it was half a hectare in size. By 13:00 on the 27th of June, it was under control. Fire 41 was declared out at 12:00 on the 28th. The final size of the fire was three hectares (OMNR, 1995a).

The fire was presumed to have been ignited at a scarred tree on the hillside. It burned in mature timber (Conifer greater than 80%, 76-100% crown closure) and on the edge of a Non-Productive area. The fire was presumably ignited at the edge of a sparsely vegetated rock outcrop. The wind was out of the southwest, which would likely have pushed the fire up the hill through the relatively poor fuel of the hillside. The ground slopes gently east-northeast upward away from the conifers (OMNR, 1983). Table 9 shows the relative frequency of the fuels in the immediate vicinity, and Figure 16 shows the arrangement of the forest in the area.

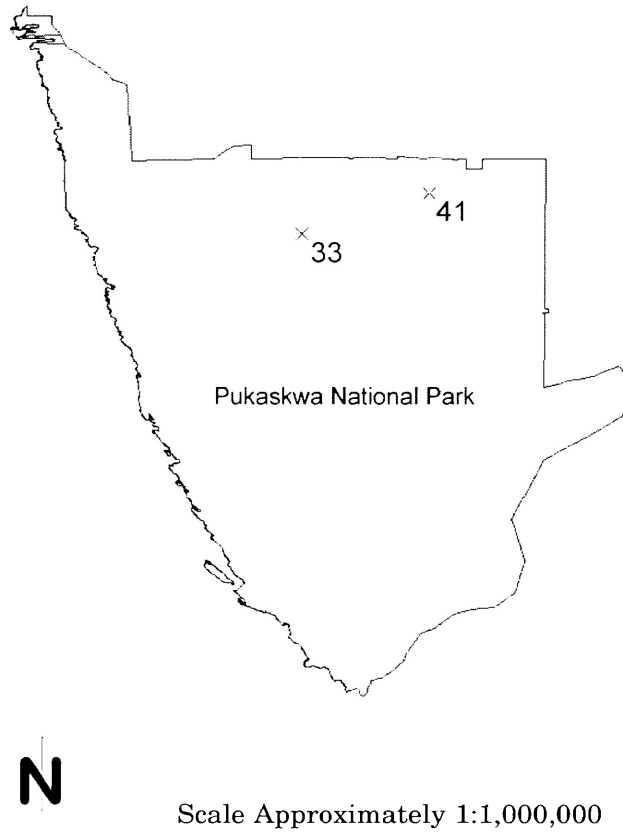


Figure 15 - The locations of the two fires discussed in the text in relation to the Park boundary. The fires were fire 33 and fire 41. They were both reported in June, 1995.

Table 8 - Soldier Mountain weather station daily data at noon for the period from June 15 to June 30, 1995. FFMC is Fine Fuel Moisture Code. DMC is Drought Moisture Code. SLP is Sea Level Pressure measured at Wawa Airport. 101.3 is the nominal "normal" pressure.

Date	Temperature (° C)	Relative Humidity (%)	Wind Azimuth	Wind Speed (km/h)	Rain (mm)	FFMC	DMC	SLP (kPa)
June-15	22.6	45.2	207	12.3	0.0	88.3	35.5	102.2
June-16	25.0	40.6	229	16.5	0.0	89.7	39.6	102.3
June-17	26.6	55.8	225	16.6	0.0	89.2	42.8	102.2
June-18	30.0	47.4	272	9.3	0.0	89.5	47.1	101.8
June-19	31.8	33.5	298	5.9	0.0	92.1	52.9	101.6
June-20	20.7	47.7	85	13.5	0.0	90.3	55.9	101.8
June-21	24.2	35.4	211	7.2	0.0	90.7	60.2	102.0
June-22	26.7	43.0	214	10.4	0.0	90.7	64.4	102.0
June-23	27.1	54.7	220	11.5	0.0	89.6	67.8	101.7
June-24 [†]	28.7	46.1	202	7	0.0	89.6	72.0	101.3
June-25 [‡]	18.1	77.3	81	18.7	4.2	62.2	50.9	101.6
June-26	22.1	52.7	83	8	0.0	80.4	53.8	101.8
June-27	21.2	75.9	146	15.8	26.2	48.6	22.5	101.6
June-28	18.7	89.6	151	13	0.0	59.9	23.0	101.3
June-29	17.7	94.6	165	9	1.2	55.4	23.3	101.1
June-30	15.7	97.7	169	11.4	0.3	57.4	23.4	101.0

[†] Fire 33 start

[‡] Fire 41 start

Table 9- Fuel types in a 400 ha square around the reported location of Fire 41. Data was derived from classified satellite imagery (Pukaskwa National Park, 1995).

Fuel Type	Hectares	Percent
Conifer>80%,76-100% Crwn Clos.	71	15%
Conifer>80%,51-75% Crwn Clos.	60	12%
Conifer>70%,25-50% Crwn Clos.	68.1	14%
MixedConifer>50%,25-50% Crown	24.1	5%
MixDecid>50%,25-50% Crown Clos	0.5	0%
Non-Productive	217.1	44%
Water	47.5	10%

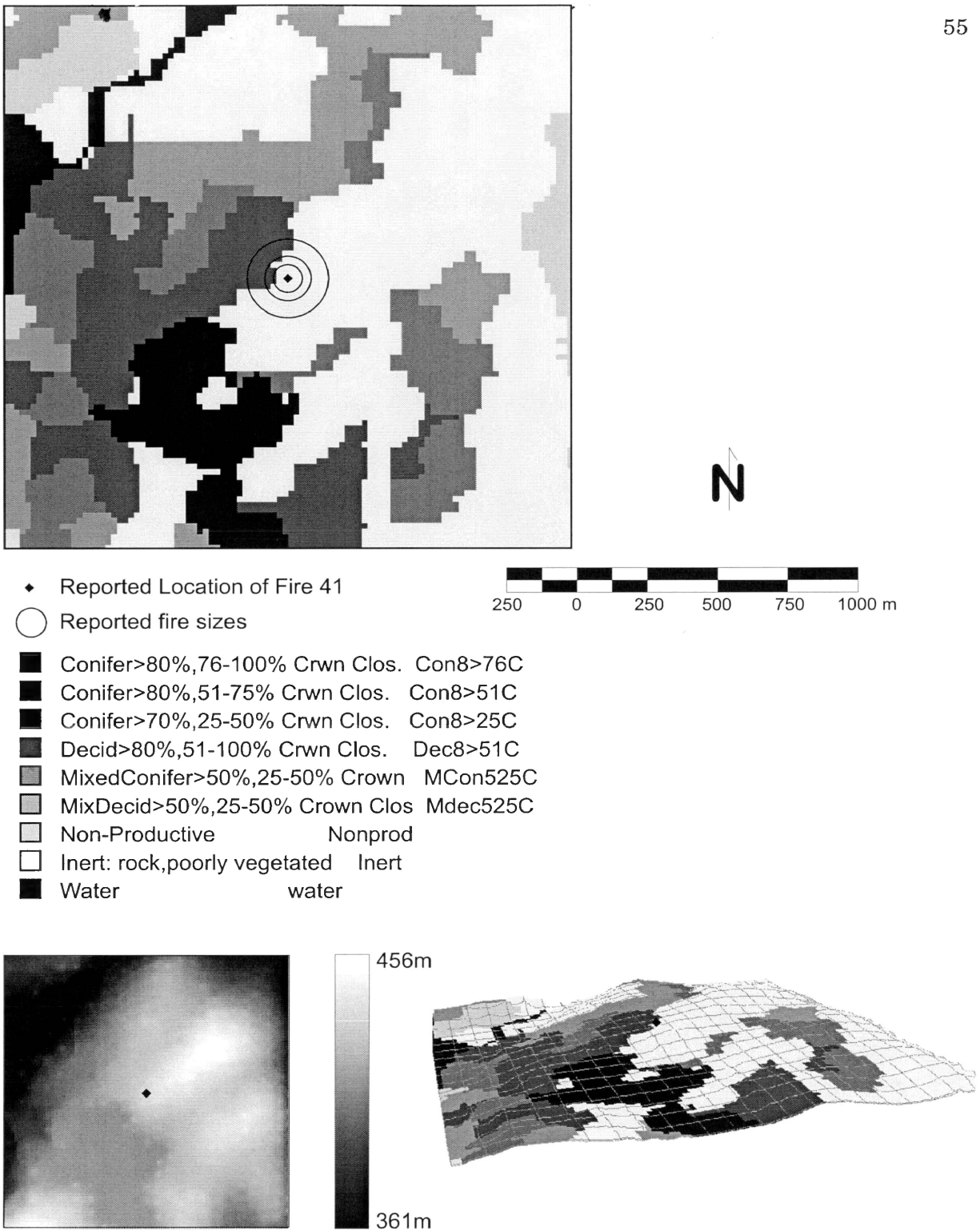


Figure 16 - The arrangement of forest types and topography near Fire 41. The forest fuel types are shown to the top left, the topography to the lower left, and a perspective view of the area to the lower right. The area shown is a 4km² square around the location of the reported fire. The circles represents the estimated area the fire attained. The circles do not represent the fire perimeter, but do represent the area as a circle. The outermost circle shows the final size. The innermost shows size at report. The middle circle shows the size at Initial Attack. The diamond shows the reported location.

The area burned by Fire 41 was most recently burned in the Oiseau Bay fire of 1936 (Street and Alexander, 1980). That fire was the largest in Ontario that year, stretching from outside the Park to the east nearly to Lake Superior. It was 47,206 hectares in area. It, too was presumed to have been started by lightning. In the 1950 Forest Resource Inventory, the area was described as “Recently Burned” (Abitibi Power and Paper Company, 1950).

There were 12 lightning strike records within 5 km of Fire 41 in the month preceding Fire 41, all the night before. These strikes are consistent with the statement on the fire report that a lightning storm had passed through the area the night before. Given the accuracy expected of the lightning detector system, no specific strike record can be presumed to have been the one that ignited this fire.

The strikes near Fire 41 ranged in strength from 4 to 8, with a mean of 5.2. All the strikes were of negative polarity. The strongest strike was recorded 2.8 km away. There were three closer strike records, at strengths of 5, 5, and 6. The closest was 400 m away.

Fire 33

Fire 33 was near UTM coordinates 578500, 5361500. It was first reported June 24 at 17:01. By the time it was first attacked at 17:45 the same day, it was 0.1 hectare in size. By 08:00 on the 25th of June, it was under control. Fire 33 was declared out at 09:00 on the 1st of July. The final size of the fire was 0.1 hectares (OMNR, 1995b).

The fuel complex of Fire 33 was described in the fire report as “non-forested” (OMNR, 1995b). In the area of the fire were non-productive area, areas that were primarily coniferous, and areas that were mainly deciduous (Table 10). The arrangement of different fuels can be seen in Figure 17.

The fuel in the immediate vicinity of Fire 33 was not burned in any of the recorded fires in the last 70 years. It was on the periphery of the Oiseau Bay Fire of 1936. The 1950 FRI (Abitibi Power and Paper Co., 1950) describes the fuels as Aspen, Birch, Spruce, and some Balsam Fir. The age class was IV, representing 60-80 years old. The area to the North and East of the fire report, which is now primarily coniferous, was described as recently burned.

There were no lightning strike records within 10 km of this fire in the month before this fire. There is a possibility that the strike was undetected. If there were no strikes in the area for a month, then the possibility must be raised that a fire smouldered undetected for that month.

Table 10- Fuel types in a 400 ha square around the reported location of Fire 33. Data was derived from classified satellite imagery (Pukaskwa National Park, 1995).

<u>Fuel Type</u>	<u>hectares</u>	<u>percent</u>
Conifer>80%,76-100% Crwn Clos.	7.04	2%
Conifer>80%,51-75% Crwn Clos.	92.32	23%
Conifer>70%,25-50% Crwn Clos.	43.92	11%
Decid>80%,51-100% Crwn Clos.	111.72	28%
MixedConifer>50%,25-50% Crown Clos	29.36	7%
MixDecid>50%,25-50% Crown Clos.	47.36	12%
Non-Productive	32.16	8%
Water	36.12	9%

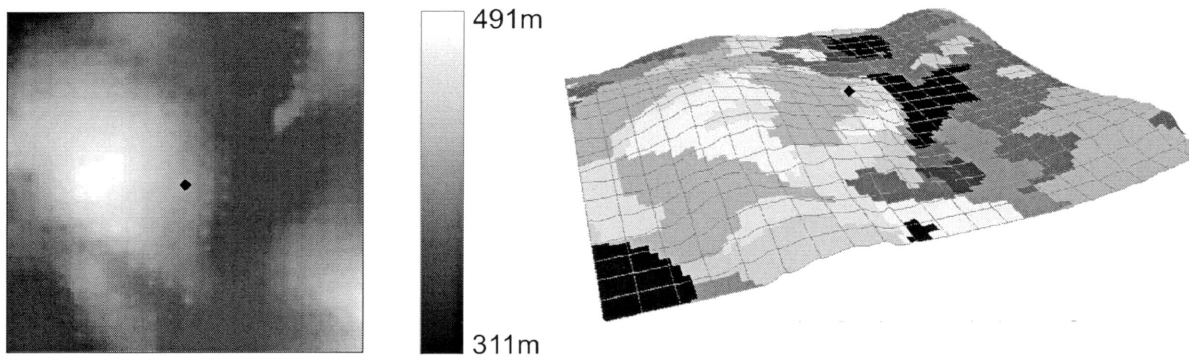
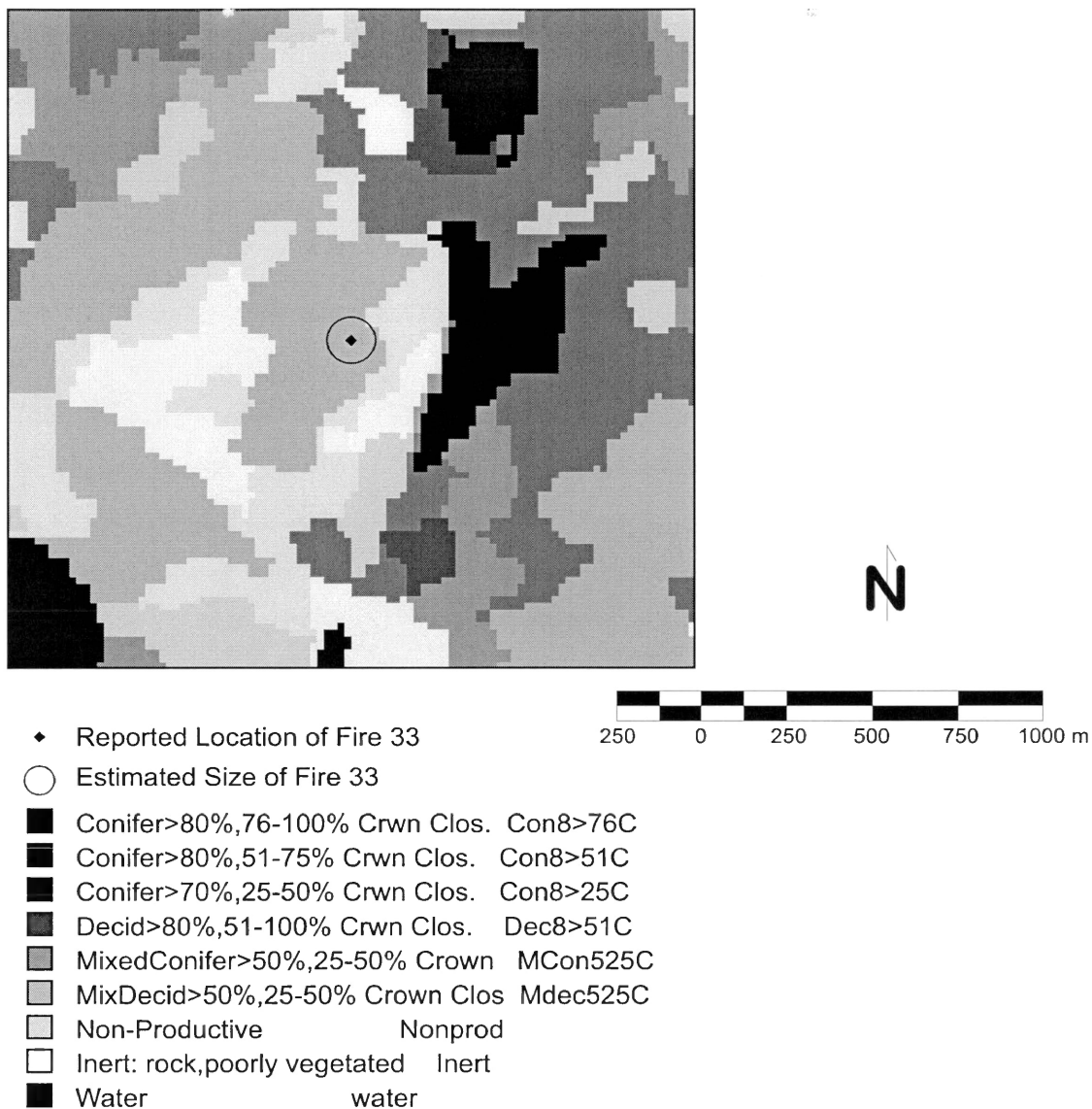


Figure 17 - The arrangement of forest types and topography near Fire 33. The forest fuel types are shown to the top left, the topography to the lower left, and a perspective view of the area to the lower right. The area shown is a 4km² square around the location of the reported fire. The circles represents the estimated area the fire attained. The circles do not represent the fire perimeter, but do represent the area as a circle. The outermost circle shows the final size and size at report. The diamond shows the reported location.

Discussion and Conclusions

Informal Examination

The informal examination exposed a minor discrepancy in the data concerning the frequency of even strength scores and odd strength scores for the lightning strikes. There was a significant difference between the number of even- and odd-strength strikes. There is no reason to expect that there should be more odd-strength strikes than even-strength strikes. This is presumably an artifact of the LDS network as implemented in Ontario. This matter probably does not materially affect the use of lightning strike data in further work, but it is something that should be accounted for in a modelling environment.

The accuracy level of the LDS system warrants some critical examination. There has been no published accuracy assessment of the Ontario system. Based on the published experience in other provinces in Canada, and other jurisdictions worldwide, between 60% and 70% of lightning strikes are detected. The range of detector system efficiency can be quite wide. Within the scope of fire detection, this relatively low rate of detection is acceptable, because the likelihood of fire is so low, and lightning detection is used to direct spotting aircraft, which then detect the fire.

The detector efficiency has been assumed to be uniform across the landscape within this study. That suggests that the detected strikes represent an unbiased sample of the strike population. This is a reasonable assumption given that the range of distances from LDS system detectors to points in the Park is reasonably uniform. At a geographic extent an order of magnitude higher, this assumption may not hold. If this type of examination were to be conducted at, for example, a provincial scale, a variability on detector efficiency should be expected, and calculated.

Section 1 - Where?

There is an effect of landscape characteristics on the probability of lightning strikes. The presence of Lake Superior has a significant effect, which confounds the analysis for certain other analyses.

The fact that there is a higher probability of lightning strikes close to Lake Superior seems intuitively reasonable. There is a change in the surface over which the air is moving, both in temperature and in texture. Some turbulence might reasonably be expected. This could cause a greater likelihood of thunder clouds, which could result in lightning strikes. The effect of this will inevitably confound analysis with the ecodistricts or the topography.

An effect of elevation is apparent, but is confounded by the effect of the proximity of Lake Superior. The elevation shows a non-intuitive negative relationship with the probability of lightning strike. This is probably caused by the negative correlation of elevation and proximity to Lake Superior. The elevation effect could, presumably, be separated from the effect of the lake's proximity. This would require the assumption of a model that included an effect of each landscape characteristic in some mathematical relationship. Whether it would be a multiplicative effect or an additive effect, or some other is not obvious from the system in question.

There is some effect on lightning probability by ecodistrict. The ecodistricts are quite strongly associated with the proximity of Lake Superior. The distribution of ecodistricts cannot be separated from their proximity to the lake.

The peak topography analysis shows a pattern that is intuitively reasonable. The peaks seem to get hit more than other areas. The peaks do not seem to be correlated with the distance from Lake Superior, and this is probably an indicator that this measurement is not affected by the dominating effect of the distance from Lake Superior. The strong difference between this result and the result for elevation suggest that the elevation analysis is confounded.

The vegetation analysis shows an effect of vegetation on strike probability. Certain vegetation types were more likely to be hit than others. The primarily coniferous areas have a higher probability of being struck by lightning than primarily deciduous areas. This may be related to the dominance of conifers in areas of high lightning activity, or it may be a real effect. Van Wagendonk (1991) found an effect of vegetation in a similar study, but discarded it because of the effect of mountain topography on the vegetation. He determined that the vegetation was not a causative agent, but was highly correlated with the causative agent elevation.

The difference in spatial precision levels between the lightning and the vegetation datasets might suggest that the vegetation analysis may not be appropriate. The errors in the lightning data are enormous compared to the scale at which the vegetation layer changes. The link shown here between vegetation and lightning strike probability is not to be given too much weight without substantial further work to confirm that there is a real correlation. The same might be said for the elevation analyses, but at a lower level of caution, given the much smoother pattern in the elevation map than in the vegetation map.

Human-dominated areas also show a higher probability of being struck than other areas. This might be related to the electrical equipment maintained in human-dominated areas.

With respect to planning a fire program for Pukaskwa National Park, these effects should be considered, at least to a degree. The higher likelihood of strikes in conifers, and near Lake Superior should inform the decisions to light prescribed burns, and plan “Natural Prescribed Fire Zones”. This knowledge should be balanced by the knowledge of higher rainfall near the lake.

The very low frequency of fire ignition reported by others (Kourtz and Todd, 1992) should also inform decision-making. The likelihood of any individual strike igniting anything is quite low. The selection of individual prescribed-burn sites should probably not be affected by any consideration of matching to the individual strikes recorded by the lightning detection system.

Section 2 - When?

These analyses of the concurrence of lightning with weather indices shows that there is a low-moderate frequency of days where a fire is likely to be able to be ignited and then survive to detection. Lightning seems to happen almost entirely at low values of the indices. The one storm that did happen at high values of the two indices probably caused a fire.

The weather probability density graphs in Figure 14 show a pattern of weather that is frequently not conducive to fire. The fine fuels may frequently be dry enough, as shown by the range of FFMC that the probability density clouds occupy. The coarser fuels take longer to dry, and so are more frequently too wet.

The lightning probability density graphs in Figure 14 show that lightning happens in

low-DMC weather. The single spot and slight cloud visible in Figure 14 (i) show that lightning inland occasionally happens at higher values of the DMC. This may be due to a difference in the pattern of storms between inland and coastal areas.

The storm event that is visible as a dense blob at high index values in Figure 14 (i) is presumably the storm that ignited Fire 41. The fact that this storm happened at high index values allowed lightning from that storm to ignite fires. The fact that the other two weather stations did not show a group of lightning strikes at these values suggests the degree to which a storm can be localized. It also suggests that the network of weather stations should include inland points like Soldier Mountain, and that reliance on coastal weather stations for analysis of weather and lightning patterns in the vicinity may not be appropriate. This might be an issue for the investigation of fire frequency and weather patterns in the period before the Park's weather stations were set up.

Section 3 - Fires

The investigations of these two fires points out two significant issues with respect to using LDS data for fire prediction. The first issue is the precision of fire location data reported by the fire crews. The second issue is the performance of the LDS system at detecting the strikes that lit the fires.

The fire reports for Fire 33 and Fire 41 both contain a coordinate at which the fire was located. The coordinates of both fires have been estimated to be within one kilometer of the actual site of the fire. In both cases, the Easting and the Northing end in 500. A look through other fire reports suggests this is the level of accuracy expected of the fire crews. To be able to use inventory data to predict likelihood of ignition in a location in the forest, more precise location of fires is required to use as check data for the model. These data are also too imprecise to do fire spread modelling properly, since the initial condition of the fuel immediately surrounding the fire cannot be determined easily.

To give a sense of scale for the imprecision of the fire location data, refer to Figures 16 and 17. The squares in Figures 16 and 17 are 2 x 2 km, centred on the fire locations reported in the fire report. The middles of the sides of the square are 1 km away from the centre of the square. The level of precision in the fire reports is 1km. In both cases, the forest condition at the actual location of the fire is very difficult to determine, given the variability of the

vegetation complex at a scale of 1 km.

The low level of precision cannot be changed for historical data, but future fire reports could be reported with greater precision. A Global Positioning System (GPS) receiver might be available for mapping the fire. The estimated ignition location would be relatively easily located if it can be identified. In the case of the two fires here, which were much smaller than a hectare at initial attack, a good guess (within 10's of meters) can be made of the ignition location.

The LDS did not detect a lightning strike in the area of Fire 33 in a reasonable time before the fire became visible, even though the fire report mentions a lightning storm moving through the area the night before. This suggests that either the LDS network is too sparse for this sort of work, or that the LDS computer miscalibrated, and is rejecting many more strikes than it should. Further investigation is needed, however. It is also possible that a single direction finder in the LDS network is not operating correctly, which is causing the incorrect rejection of some strikes, or the incorrect location of some strikes. This effect was documented in Alberta by Nimchuk (1990).

Before modelling the fire ignition probabilities from the existing lightning data, an accuracy assessment needs to be performed on the lightning location data. The two fires considered here were ignited (presumably) by lightning strikes. The fire for which potential strikes could be identified had 12 strikes within 5 km. Although there is a significant expectation of missed strikes, about 40%, there is an unknown level of spatial accuracy of the data. The data are sufficiently accurate for the original purpose of the detector network, but may not be sufficiently accurate for the purposes of comparison with elevation or vegetation patterns.

The data, with these two issues, are available for modelling the conditions under which fires are ignited. All that is required is a larger number of fires. This could be achieved by using a larger geographic extent, or by increasing the number of years in which fires have happened.

Suggestions for Possible Future Research

Probability of Fire Ignition

To further examine the effect of lightning density on fire ignitions, more fire ignitions must be examined. To do that, a larger temporal or geographical context is required. More ignitions could lead to a statistical procedure that might bring a significant pattern to light.

The investigation of what conditions are good predictors of fire ignition from lightning in Pukaskwa could be developed further. The LDS data from as early as it was available until the present could be compared with fire ignitions in some statistical way. Flannigan and Wotton (1991) did something similar, only with a larger geographic area, and for one year. For the Pukaskwa area, this could be performed over multiple years for which there is lightning data. This would probably yield a limited number of fire ignitions within the Park, as lightning data is only available since about 1987.

Another study might be undertaken similar to that of Flannigan and Wotton (1991) using a larger geographic area than just the Park. This proposed study would examine fire ignition patterns from lightning for a geographic region including Pukaskwa National Park. Kernel methods could be used for the classification of the fire ignitions, so that multivariate normalcy of all the input data need not be assumed. Input data might include topography, lightning occurrence, fire history and reports, vegetation information and weather.

Strikes on Exposed Ledges

One of the questions discussed during the formation of ideas for this report was whether lightning hits exposed ledges more frequently than the valley below or the upland behind. This discussion was motivated by the observation of charred wood on these exposed ledges, but not in the forest behind the ledges. There is some basis in the lightning literature to believe it is possible that there is a locally increased likelihood of strikes on these exposed corners. This is derived from the idea that the process of attachment of the leader to the ground happens at a scale of 10's of metres. A 100m cliff could influence the process of

lightning attachment to the ground enough to significantly increase the probability of lightning strikes on the ledge, and cause a “lightning shadow” below. To investigate this further, lightning detection needs to happen with a much higher positional accuracy than was available for this study. A higher-density network of direction finders, of whatever type, would allow higher accuracy of lightning location. A class map could be developed from the elevation data showing these ledges, and then an analysis similar to the one in this report could take place. This would require significant resources to create a high-density lightning detection network, and would probably not yield much better information than the observations available now from personal examination of these exposed ridge corners.

References

- Abitibi Power and Paper Company, 1950. Inventory Surveys. Maps provided on CD-ROM by Pukaskwa National Park.
- Baylor University, 1997. GRASS GIS, v. 4.2. Available from <http://www.baylor.edu/~grass>. Checked March 21, 1998.
- Brown, K.M. 1995. Design and analysis of experiments. K.M. Brown: Thunder Bay, ON. 228 pages.
- Crofts, M. 1998. Personal Communication - Correspondence dated December 12, 1998.
- Epanechnikov, V.A. 1969. Non-parametric estimation of a multivariate probability density. *Theory of Probability and its Applications*. 14:153-158.
- Flannigan, M.D. and B.M. Wotton. 1991. Lightning-ignited forest fires in northwestern ontario. *Can. J. For. Res.*, 21:277-287.
- Forestry Canada. 1992. Development and structure of the canadian forest fire behaviour prediction system. Forestry Canada: Hull, PQ. 63 pages.
- Frandsen, W.H. 1987. The influence of moisture and mineral soil on the combustion limits of smouldering forest duff. *Can. J. For. Res.*, 17: 1540-1544.
- Free Software Foundation. 1997. GNU C, version 2.7.2.2. Available at <ftp://ftp.cs.ubc.ca/mirror2/gnu/gcc2.7.2.2.tar.gz>. Checked October 7, 1998.
- Geomatics. 1996. Pukaskwa national park ecosystem conservation plan. Geomatics: Ottawa.
- Gilbert, D., B. Johnson, C. Zala, 1987. A reliability study of the lightning locating network in British Columbia. *Can. J. For. Res.* 17: 1060-1065.
- Heathcott, M. and M. Crofts. 1997. Forest Fire Management Plan, Pukaskwa National Park Department of Canadian Heritage - Parks Canada. 23 pp.
- Herodotou, N. 1990. Study of peak currents due to lightning in Ontario using an LLP system, M.S. Thesis, Univ. of Toronto, Toronto, ON. 215 pages.
- Hojo, J., M. Ishii, T. Kawamura, F. Suzuki, H. Komuro, and M. Shiogama. 1989. Seasonal variation of cloud-to-ground lightning flash characteristics in the coastal area of the Sea of Japan. *J. Geophys. Res.* 94:13207-13212.
- Huse, J. and K. Olsen. 1984. Some characteristics of lightning ground flashes observed in Norway. In *Proceedings of the International Conference on Lightning and Power Systems*, 5-7 June, 1984, London. Institution of Electrical Engineers, London. 1984. pp. 72-79.
- Idone, V.P., A.B. Saljoughy, R.W. Henderson, P.K. Moore, and R.B. Pyle. 1993. A reexamination of the peak current calibration of the national lightning detection network. *J. Geophys. Res.* 98:18323-18332.
- Jones, M.C., J.S. Marron, and S.J. Sheather. 1996. A brief survey of bandwidth selection for density estimation. *J. Amer. Stat. Assoc.* 91:401-407.

- Lawson, B., O.B. Armitage, and W.D. Hoskins, 1996. Diurnal variability in the fine fuel moisture code: Tables and computer source code. FRDA report 245. Canadian Forest Service. 83 pages.
- Lawson, E.J.G., and A.R. Rodgers. 1997. Differences in home-range size computed in commonly used software programs. *Wildl. Soc. Bull.* 25:721-729.
- López, R.E., M.W. Maier, and R.L. Holle. 1991. Comparison of the signal strength of positive and negative cloud-to-ground lightning flashes in northeastern Colorado. *J. Geophys. Res.* 96:22307-22318.
- Kenward, R.E., and K.H. Hodder, 1996. RANGES V: an analysis system for biological location data. Inst. Terrestrial Ecol., Furzebrook Res. Stn., Wareham, UK. 66pp.
- Kourtz, P., and B. Todd, 1992. Predicting the daily occurrence of lightning-caused forest fires. Information Report PI-X-112, Petawawa National Forestry Institute, Forestry Canada. 18 pages.
- Mach, D.M. and W.D. Rust. 1993. Two-dimensional velocity, optical risetime, and peak current estimates for natural positive lightning return strokes. *J. Geophys. Res.* 98:2635-2638.
- Nash, C., and E. Johnson, 1996. Synoptic climatology of lightning-caused forest fires in subalpine and boreal forests. *Can. J. For. Res.*, 26: 1859-1874.
- Nimchuk, N. 1990. Ground-truthing of LLP lightning location data in Alberta. In *Proceedings of the 10th conference on fire and forest meteorology*, Society of American Foresters: Bethesda, MD, USA. pp. 33-40.
- National Climatic Data Center. 1997. Global surface summary of day. <http://www.ncdc.noaa.gov/ol/climate/online/g sod.html>, downloaded November 11, 1997.
- Natural Resources Canada. 1998. Canadian geographic names. Available at <http://GeoNames.NRCan.gc.ca/english/>. Checked May 5, 1998.
- Noggle, R., E. Krider, D. Vance, and K. Barker. 1976. A lightning direction-finding system for forest fire detection. In *Proceedings of 4th National Conference on fire and forest meteorology*. USDA Forest Service General Technical Report RM-32.
- OMNR, 1996. Lightning strike data, from 1994, 1995, 1996, for 47°-49°N, 84.5°-86.5°W. Provided by Sid Jordan, Weather Briefing Technician, Aviation, Flood & Fire Management Branch, Ontario Ministry of Natural Resources, Sault Ste Marie.
- OMNR, 1995a. Fire report, Fire 41. Document on file at Pukaskwa National Park.
- OMNR, 1995b. Fire report, Fire 33. Document on file at Pukaskwa National Park.
- OMNR, 1983a. Ontario Base Map 2016590053600.
- OMNR, 1983b. Ontario Base Map 2016570053600.
- Orville, R.E.. 1994. Cloud-to-ground lightning flash characteristics in the contiguous United States: 1989-1991. *J. Geophys. Res.* 99:10833-10841.
- Orville, R.E. and A.C. Silver. 1997. Lightning ground flash density in the contiguous United States: 1992-95. *Mon. Weather Rev.* 125: 631-638.

- Passi, R.M., and R.E. López. 1989. A parametric estimation of systematic errors in networks of magnetic direction finders. *J. Geophys. Res.* 94:13319-13328.
- Perlman, G. 1987. Translations of TOMS algorithms into C. <ftp://ftp.cdrom.com/.3/netlib/a/perlman> . Checked November 17, 1997.
- Petersen, W.A. and S.A. Rutledge. 1992. Some characteristics of cloud-to-ground lightning in tropical Australia. *J. Geophys. Res.* 97:11533-11560.
- Pukaskwa National Park, 1995. Classified satellite imagery, on file. Classification performed at LU-CARIS, Lakehead University.
- Rakov, V.A., M.A. Uman, and R. Thottappillil. 1994. Review of lightning properties from electric field and TV observations. *J. Geophys. Res.* 99:10745-10750.
- Remsoft Inc., 1996. WeatherPro Software and User's Guide Version.1.01. Remsoft Inc. Fredericton, New Brunswick. 185pp.
- Rosenblatt, M. 1956. Remarks on some nonparametric estimates of a density function. *The Annals of Mathematical Statistics* 27:832-837.
- Runyon, R. P., A. Haber. 1988. Fundamentals of behavioral statistics, 6th ed. Random House: New York. 494 pages.
- Seaman, D.E. and R.A. Powell, 1996. An evaluation of the accuracy of kernel density estimators for home range analysis. *Ecology* 77: 2075-2085.
- Shindo, T., and M.A. Uman, 1989. Continuing current in negative cloud-to-ground lightning. *J. Geophys. Res.* 94: 5189-5198.
- Silverman, B.W. 1986. Density estimation for statistics and data analysis. Chapman and Hall: London. 175 pages.
- Street, R. B., and M. E. Alexander, 1980. Synoptic weather associated with five major forest fires in Pukaskwa National Park. *Atmos. Envir. Serv., Ont. Reg. Int. Rep. SSD-80-2.*
- Tufto, J. 1994. Kernel program for DOS. Available from: Tom's Wildlife Telemetry Clearinghouse, <http://www.uni-sb.de/philfak/fb6/fr66/tpw/telem/dataproc.htm#hr> . Checked March 4, 1998.
- Uman, M.A. and E.P. Krider. 1989. Natural and artificially initiated lightning. *Science* 246:457-464.
- USA-CERL. 1995. GRASS GIS, release 4.1, patch level 5. <http://moon.cecer.army.mil/pub/grass/release/binary/linux> . Checked November 17, 1997.
- Van Wagtendonk, J., 1991. Spatial analysis of lightning strikes in yosemite national park. In *Proceedings of the 11th conference on fire and forest meteorology, Society of American Foresters: Bethesda, MD, USA.* pp. 605-611.
- Van Wagner, C., 1987. Development and structure of the canadian forest fire weather index system. Canadian Forestry Service: Ottawa. 45 pages.
- Van Wagner, C., and T.L. Pickett. 1985. Equations and fortran program for the canadian forest fire weather index system. Canadian forestry service forestry technical report 33. 63 pages.

Wand, M.P., and M.C.Jones. 1995. Kernel smoothing. Chapman and Hall: London. 215 pages.

Worton, B.J., 1989. Kernel methods for estimating the utilization distribution in home-range studies. *Ecology*, 70:164-168.